The need for regulation of climate subsystems

Romain Fillon*[1,2] and Céline Guivarch[2]

[1]*Paris-Saclay Applied Economics, Graduate School of Economics & Management, INRAE, Université Paris-Saclay, France*

[2]*CIRED, Ecole des Ponts, AgroParisTech, EHESS, CIRAD, CNRS, Université Paris-Saclay, France*

October 29, 2024

Abstract

Understanding stochastic interactions between climate change, the macroeconomy and Earth subsystems with non-linear, self-sustaining and debated dynamics is a major challenge with implications both for global climate policy and regional subsystem's management. We study Earth subsystems with three properties: their dynamics have an impact on climate change, climate change has an impact on their dynamics and their dynamics are not entirely determined by climate change. We analytically derive the three channels through which interactions between subsystem's idiosyncratic risk and aggregate climate risk over intertemporal welfare affect optimal climate policy. First, subsystems have direct scaling effect through their expected feedback on global climate. Second, perturbations in the subsystem caused by carbon emissions reduce its long-term survival and therefore affect intertemporal welfare because of future feedbacks on global climate. Third, subsystems have various insurance values. We also highlight how an explicit reduced-form subsystems's geophysical dynamics improves their management, taking into account the changing ability of the subsystems to self-perpetuate over time: we introduce the social cost of the dynamic subsystem (SCDS). We apply our framework in a calibrated stochastic quantitative model of the Amazon rainforest whose fate is fiercely debated. In our benchmark quantitative specification, an endogenous and explicit modeling of the Amazon rainforest implies a 15% risk premium on the social cost of carbon (SCC) at the global scale and a SCDS that is worth 16% of the standard stochastic SCC. These results imply that a 24% increase in the marginal value of a tCO_2 stored in the rainforest should be applied in local cost-benefit analysis.

Keywords : dynamic stochastic climate-economy model, robust environmental policy, Amazon rainforest, climate tipping elements, scientific uncertainty, risk.

*Corresponding author: rfillon@protonmail.com.

Introduction

The Earth and human societies are complex systems with non-linear stochastic dynamics, entangled through time and space. Our knowledge of the climate system and the interactions of its components has made significant progress, even if it remains subject to scientific debate. Meanwhile, economic models usually rely on a stylized representation of climate change where feedbacks between global climate change and subsystems such as tropical rainforests are either omitted, deterministic or modeled as a generic catastrophe with no geophysical representation, even in reduced form. Yet, impacts of climate change on these subsystems are stochastic: for instance, the law that describes how more frequent occurence of droughts under changing climate might affect tree losses in the Amazon rainforest is not deterministic (Anderson et al., 2018). Furthermore, the possible collapse of these subsystems is more complex than a probability defined *ex ante*: because of vegetation-rainfall feedbacks (Zemp et al., 2017), a decrease in forest cover could for instance yield an abrupt partial dieback that is not a linear function of an additional CO_2 emission or an additional hectare of deforestation. In this paper, we analyze and quantify how moving beyond these simplifications yields fruitful insights for decision-making regarding adaptation and mitigation under a changing climate endogenous to our economic activities.

We focus on climate subsystems that have three properties. First, global climate change has an impact on their dynamics, e.g. through changes in the drought regime under a changing climate for the Amazon rainforest. Second, our subsystems have an impact on global climate change: indeed, rainforests can for instance store and release carbon. Both impacts can be positive or negative. Third, subsystem's dynamics cannot be simply deduced from climate change, because of inertia, self-sustaining dynamics or feedback effects: for instance, the Amazon rainforest recycles part of its precipitation to feed its own growth through evapotranspiration. Examples of Earth subsystems are for instance climate tipping elements (Armstrong McKay et al., 2022). Examples of Earth subsystems of relevance to this study also include other subsystems that do not have tipping behavior, such as the South-Eastern Asian rainforest and its feedback on the global carbon cycle or El Niño La Niña and its impact on intra- and inter-annual natural climate variability.

We build a dynamic climate-economy model, extending a well-established literature studying optimal policy under climate risks (Golosov et al., 2014; Cai and Lontzek, 2019; Folini et al., 2024). In comparison with previous work, we explicitely include a stylized climate subsystem with its own

dynamics as a state variable of our program, e.g. the current forest cover of the Amazon, and model its stochastic interactions with climate change. Introducing a stylized subsystem has important implications both for optimal climate policy and regional subsystem management.

First, a key question for optimal climate policy is to know if and to what extent subsystem's idiosyncratic risk affects aggregate climate risk bearing over intertemporal welfare. Indeed, the feedbacks brought by these subsystems on global climate might not have the same social value for different states of the world where they might occur, which depend on their own dynamics, its interaction with climate change with possible thresholds and the timescales over which transitions to different states occur for the subsystem. Furthermore, while some subsystems are expected to decrease global and regional temperatures if global temperature increases, e.g. southern boreal forest dieback or Labrador-Irminger seas/Subpolar Gyre oceanic convection collapse, some others are expected to increase temperatures under warming climate, e.g. abrupt permafrost thawing or Arctic winter sea ice collapse (Armstrong McKay et al., 2022): the subsystems have different insurance value with respect to intertemporal utility. Without loss of generality, we analytically derive the channels through which our subsystem changes optimal policy using value function decomposition. As in the climate economics literature inspired from asset pricing (Dietz et al., 2018; Lemoine, 2021; Van den Bremer and Van der Ploeg, 2021), we depict how the social cost of carbon (SCC) is affected by different components when accounting for climate risks, thinking of the subsystem as a climate asset that can increase or decrease aggregate risk of the wider climate portfolio.

We show that an Earth subsystem affects climate policy through three channels. First, it scales multiplicatively the standard certainty equivalent and precautionary channels driving SCC depending on how and how much its feedback affects global climate change. Second, a marginal change in the subsystem's state brought by a marginal emission today yields an additive change in optimal policy because of the marginal impact of this change in the future dynamics of the subsystem on the continuation value. Third, an insurance channel, i.e. a 'subsystem beta', increases the SCC if the subsystem has a larger feedback effect on global climate change in the states of the world where a marginal emission has the largest impact on intertemporal welfare.

Second, an important question for optimal subsystem management is to analyse and quantify how a marginal variation in the state of the subsystem affects intertemporal welfare. Indeed, a marginal change in the subsystem's state has a first-order impact on optimal policy as it changes global temperatures, for instance because of carbon releases from the Amazon rainforest. But a marginal change in the subsystem's state also has a second-order impact on optimal policy as it affects the growth of

the subsystem in all future periods. We introduce the social cost of the dynamic system (SCDS): it measures in present monetary terms the intertemporal social cost of a marginal decrease in the subsystem's state today, which captures the extent to which the future subsystem's ability to self-perpetuate changes with a marginal change in its current state. The decrease in the subsystem's ability to self-perpetuate increases aggregate risk bearing over intertemporal welfare through future feedbacks of the subsystem on global climate.

We apply our framework to the debated fate of the Amazon rainforest in a stochastic quantitative model. We focus solely on its value as a carbon stock. This subsystem has a major regulating function for the Earth. At the global scale, it acts as a carbon sink of $\sim 123 \pm 23$ GtC biomass (Malhi et al., 2006). This represents a significant 39% ($\pm$ 7%) of the remaining budget to keep two chances out of three of limiting global warming to 2°C according to IPCC (Masson-Delmotte et al., 2021). The Amazon rainforest is therefore very valuable. But the Amazon rainforest is in danger as a result of human actions. A combination of forest degradation, deforestation, climate change and feedback effects may cause a partial dieback of the rainforest (Lovejoy and Nobre, 2019). The direct human impact, through deforestation and degradation, is attracting a lot of attention among economists (Balboni et al., 2023), and for good reasons. But human activities also affect the rainforest indirectly through climate change. Anthropogenic climate change is expected to change precipitation patterns, especially make extreme droughts which generate tree mortality and carbon losses (Phillips et al., 2009; Yao et al., 2022) more frequent. A ton of carbon emitted in Europe or Asia thus has an impact on the rainforest. In turn, the forest increases the damage of future climate change in Europe and Asia, as it might release carbon under changing climate. In particular, the rainforest feedback might be the largest in states of the world where cumulative emissions have the largest impact on aggregate welfare, thus increasing aggregate risk bearing over intertemporal welfare. Finally, vegetation-rainfall feedback effects limiting the recycling of water by the forest, i.e. forest's own dynamics, may magnify these human-induced perturbations (Zemp et al., 2017). This self-sustained dynamics arising from temporal autocorrelation, in which decisions in some part of the forest affect other parts because of spatial autocorrelation, is usually neglected in local cost-benefit analysis or in dynamic discrete choice approaches (Souza-Rodrigues, 2019; Araujo et al., 2020; Hsiao, 2021). Finally, the fate of the Amazon rainforest is not only risky, it is also uncertain. Aside from standard risk scenarios, where future state probabilities are known, uncertain situations are situations in which there is no unanimous probability assignment due to insufficient information or competing datasets, models, or expert opinions.

Indeed, projections of rainfall patterns under climate change differ depending on the climate model used (Kent et al., 2015). Furthermore, there are debates about whether feedback effects might yield a tipping point in the Amazon rainforest (Flores et al., 2024). We calibrate the perturbations to the dynamics of the rainforest with three components: exogenous deforestation and degradation scenarii (Aguiar et al., 2016; Matricardi et al., 2020), bias-corrected downscaled output on monthly precipitation from hydrological model MATSIRO for four ISIMIP earth system models (IPSL-CM5A-LR, HadGEM2-ES, GFDL-ESM2M, MIROC5) forced with future emissions from three different Shared Socioeconomic Pathways (SSPs) and historical observations of the impact of droughts on tree losses (Phillips et al., 2009; Yao et al., 2022). Given these calibrations, we jointly calibrate the remaining parameters of the Lotka-Volterra equation describing tipping behavior of tropical forests in Ritchie et al. (2021) to match the central estimate of the core expert probability assessment of Kriegler et al. (2009). Finally, we use both discounted expected utility and a more flexible smooth ambiguity criterion (Berger et al., 2017; Barnett et al., 2020) as a sensitivity check to measure how our collective attitudes towards risks and scientific uncertainties might affect optimal policy estimates.

Our approach yields two key methodological insights for the Amazon rainforest. First, the social cost of carbon (SCC) should include the impact that a marginal increase in cumulative emissions at the global scale has on the dynamics of the rainforest. This includes a scaling of current policy by the carbon releases from the Amazon rainforest under changing climate, an additive risk premium in the SCC from the perturbation on the present and future dynamics of the rainforest and an insurance channel, the positive 'amazon beta', because the carbon releases occur in states of the world where carbon emissions have the largest marginal impact on intertemporal welfare. Second, the social value of the Amazon rainforest as a carbon stock cannot be reduced to the amount of carbon it contains: the social cost of the dynamic system (SCDS) matters too, i.e. the cost of a marginal decrease in subsystem's state because of its reduced ability to self-perpetuate.

These methodological results yield two key policy insights. First, decision-makers should augment the social cost of carbon (SCC) from the impact of a marginal emission on the Amazon rainforest, that further releases carbon. Emitters around the world should pay for the welfare impact of their emissions: the wedge between standard SCC and SCC with endogenous amazon feedback could be leveraged to finance payment for ecosystem services for the preservation of the rainforest. In our benchmark specification, we show that this wedge represents 15% of the standard SCC under aggregate climate risk. Second, the social value given to a hectare of rainforest should not be only the standard social cost of carbon SCC, but the sum of the amazon-augmented social cost of carbon and

the social cost of the dynamic system SCDS. Indeed, a marginal decrease in the forest cover has a first-order welfare impact, as it releases carbon, but also a second-order impact on the future dynamics of the subsystem as a whole. Under our benchmark specification, SCDS represents 16% of the standard stochastic SCC. Our theoretical work can therefore be operationalized in local cost-benefit analysis of deforestation and be used in complement to the significant progress in the quantification of carbon stored at the finest scale via satellite observation. Indeed, we show that the valuation of one tCO_2 of carbon stored in the forest should be increased by 24% in local cost-benefit analysis to reflect the true risk premium on intertemporal utility that this marginal change in its state and corresponding carbon releases represent. This scaling factor corresponds to the sum of the increase in the SCC due to the endogenous modelling of the rainforest dynamics and its interaction with global climate risk, and the share of the SCDS that corresponds to the marginal impact on intertemporal utility of a marginal change in subsystem's state. We believe that our framework could be extended to other climate subsystems to inform policy decisions at the global and regional scales.

To our knowledge, we provide the first analytical study of the stochastic interactions between the macroeconomy, climate change and a climate subsystem and the first quantitative study of the Amazon rainforest in a global perspective in a dynamic stochastic climate-economy model with an explicit geophysical representation of its uncertain dynamics. We contribute to different strands of literature. First, we bridge the gap between a literature using stochastic climate-economy models with stylized climate risks, e.g. Cai and Lontzek (2019), and a literature using deterministic models with explicit geophysical dynamics, e.g. Nordhaus (2019); Dietz et al. (2021). Thus, we contribute, along with others e.g. Dietz et al. (2021), to a better understanding of the impact of climate dynamics on economic decisions. Second, we bring together complex numerical stochastic climate-economy models with analytical decompositions that allow to identify the precise channels through which climate risks affect optimal policy (Lemoine, 2021). In comparison with a prolific literature using more stylized approach where the tipping risk is a probability to switch from one qualitative state to another one (Lemoine and Traeger, 2014; Fillon et al., 2023), we have a more complex dynamics as the subsystem is a state in our dynamic program. Our decomposition also relates to the debates on the 'climate beta' (Dietz et al., 2018) and on how climate mitigation affects aggregate risk bearing on intertemporal welfare. Third, we contribute to the literature on the modeling of complex non-linear socio-ecological systems (Levin et al., 2013). Indeed, we model the catastrophic outcome as an emerging property of the dynamic system with an explicit reduced-form geophysical representation, in line with bifur-

cation theory (Ritchie et al., 2021). We depart from perturbation approaches considering small risks (Van den Bremer and Van der Ploeg, 2021), *ad hoc* probability assignments (Cai and Lontzek, 2019) or macroeconomics literature on disasters considering reversible extreme events that occur as one-off catastrophes along a smoothly evolving climate regime with fluctuations, traditionally modeled with Poisson and Wiener processes (Hong et al., 2023). Indeed, our framework allows a possible abrupt dieback of the rainforest, which raises numerical challenges: following insights from Cai (2019), we use simplicial Chebyshev polynomials and break one level of 'curse-of-dimensionality' related to approximation nodes with parallel CPU computing. Fourth, we contribute to the literature on the Amazon rainforest: in comparison with most approaches focusing on deforestation (Balboni et al., 2023), we consider the impact of climate change on the rainforest and model the dynamics of the subsystem as a whole. We take a welfarist approach at the global scale to provide estimates of the marginal value of an hectare of rainforest taking into account the impact that a marginal change has on all other parts of the forest. Finally, we contribute to the literature on robust social choice criteria for social decision-making under climate risks and uncertainties (Berger et al., 2017; Barnett et al., 2020, 2022). Beyond stochastic risk in climate and economic models, i.e. the distribution of a stochastic variable of interest within a given model, there are large scientific controversies between models, for instance on climate tipping points, their mechanisms, thresholds, timescales, for which authors provide confidence assessments (Armstrong McKay et al., 2022). The disagreements on the right modelling approaches to climate tipping elements yield debates on their possible economic consequences (Keen et al., 2022). These scientific disagreements and heterogeneous confidence in assessments on climate dynamics should be taken into account when making social choice, at least as a robustness check on our best policy estimates. Alongside a more in-depth modeling of climate risks, a key issue for public and scientific debate is indeed to provide greater flexibility in the attitudes towards these risks. Our approach allows for a clear distinction, using a two-step approach, between the purpose of the risk and our attitudes towards it.

In the first analytical part (section 1), we study through value function decomposition how our modelling approach of climate subsystems affects both global climate policy and regional subsystem's management. In the second numerical part (section 2), we apply this general framework and calibrate a dynamic stochastic climate-economy model with an explicit modelling of the Amazon rainforest.

1 Modeling approach

We build a dynamic climate-economy model, extending a common framework used in the economics literature to study optimal climate policy (Cai and Lontzek, 2019; Dietz et al., 2021). We augment the model with a stylized representation of a subsystem of the Earth system whose uncertain dynamics interacts with global climate change. We study optimal policy under two distinct social choice criteria. The first criterion is the expected utility criterion: the social planner chooses between prospects by comparing their expected utilities. The second criterion (Klibanoff et al., 2005; Hayashi and Miao, 2011) allows to disentangle preference over time, over states of the world and over scientific models of the world. We highlight analytically how the subsystem might affect optimal global climate policy and suggest a measure for optimal regional management of this subsystem.

1.1 A dynamic climate-economy model

Our model has three ingredients: the macroeconomy, climate change, and an earth subsystem. This study focuses on their dynamic interactions. The three corresponding variables are net output Y, global surface temperature T, and the current state of the dynamic subsystem relative to its initial state A. The individual dynamics of these systems might be stochastic, for example due to other economic risks such as uncertain future technological change, but we focus on stochasticity in the interactions between these dynamic systems. We do not model the interactions between the macroeconomy and the subsystem: we focus on the additional feedback the subsystem brings on global climate change. Other impacts are for instance regional health effects or loss of use and non-use values from the subsystem, but we focus on the first-order market impacts on global welfare through global climate change. Furthermore, while some subsystems have an impact via other channels, for instance rainfall changes under Atlantic Meridional Overturning Circulation (AMOC) collapse, our climate variable is global annual mean temperature. Alternative climate indicators could be used depending on the specific risk of each subsystem while keeping the same framework. Our framework also makes it possible to consider extensions, for example if several subsystems interact (Cai et al., 2016). Finally, we do not model impacts of the subsystems on regional temperature separately from global impacts, because they are of different magnitude but of the same sign. The framework could be extended to integrate this additional mechanism.

This set of assumptions leaves us with four key interaction channels between the macroeconomy, aggregate climate change and the stylized earth subsystem. First, climate change affects eco-

nomic output ($\partial Y/\partial T$) through a global damage function. Second, economic output affects global climate change ($\partial T/\partial Y$) through emissions that can be abated at a given cost and add up to a cumulative emissions stock. Average surface temperature is a linear function of this cumulative emission stock through transient climate response to cumulative emissions. Third, subsystem's dynamics affects global climate change ($\partial T/\partial A$). Finally, climate change affects the subsystem's state ($\partial A/\partial T$) through various mechanisms which can be presented in a reduced-form approach with credible geophysical dynamics and an explicit calibration. These four channels are four components through which stochastic risk affects optimal policy. The two first channels, i.e. damage uncertainty and uncertainty in the transient climate response to cumulative emissions, are already well studied in the climate-economics literature and not specific to the study of subsystems. Instead, the question of the interaction of aggregate climate risk on intertemporal welfare with idiosyncratic subsystem risk is of interest to us. The two last channels, especially the fourth and most important one which determines whether or not there will be feedbacks between global climate change and the subsystem, are usually modeled (Nordhaus, 2019; Dietz et al., 2021) as deterministic or with *ad hoc* probabilities. Furthermore, the dynamics of the subsystem itself is in general not represented, even though there are important debates and scientific uncertainty about its shape that matter for optimal social choice. We model a dynamic subsystem whose dynamics is risky, uncertain, self-sustaining (e.g. a decrease in the subsystem's state reduces its ability to self-perpetuate) and interacts with global climate risk. We focus on two sources of stochastic risk and their interaction: standard aggregate risk on the transient response of global temperature to cumulative emissions ($\partial T/\partial Y$) and idiosyncratic subsystem risk on the impact of global climate change on the subsystem ($\partial A/\partial T$).

Consider a system A whose dynamics is a function of its state and of climate change. Let us assume that ϵ summarizes the impact of climate on the subsystem through temperature. We have that: $dA/dt = f(\epsilon(T), A)$. Examples of such stylized dynamics for slow-onset (AMOC collapse) or fast-onset (forest dieback) tipping elements are given in Ritchie et al. (2021). Let us assume that this subsystem's dynamics has an impact on welfare: it can affect global climate change and economic damages. But the system has a risky dynamics, as climate impacts on the system are stochastic: $dA/dt = f(\tilde{\epsilon}(T), A)$. Furthermore, there are scientific uncertainties, for instance on the transition law f of the dynamic system or on the distribution of stochastic $\tilde{\epsilon}(T)$ linking climate change to changes in A. Different models *i* and different models *j* give different transition functions and different distributions respectively, so that: $dA_{ij}/dt = f_i(\tilde{\epsilon_j}(T), A_{ij})$. To make optimal decisions, the planner takes into account the entire stochastic distribution of each ϵ_j within each possible function f_i and

weights over the alternative models with a given aggregation rule g, so that: $dA/dt = g[dA_{ij}/dt] = g\left[f_i(\tilde{\epsilon_j}(T), A_{ij})\right]$. There are m alternative models, i.e. m alternative combinations of i and j.

1.2 Social choice criteria

Social planner maximizes intertemporal welfare under endogenous climate damages and subsystem's dynamics. The state space is $\mathcal{S}$. The state variables are $x = (A, T, Y)$. $\Gamma(x)$ is the control set. Control is μ, the abatement rate. Following Golosov et al. (2014), we assume a fixed savings rate. At time t, decision maker's information consists of history $\omega_t = \{\omega_0, \omega_1, ..., \omega_t\}$ with ω_0 given. The uncertainty is described by the random m in the set M: a discrete indicator of alternative models for the subsystem. The decision maker has a prior χ_0 over m. Each m gives a probability distribution π_m over the state space. The posterior χ_t and conditional likelihood $\pi_{m,t}$ are obtained by Bayes' rule.

Discounted expected utility Under expected utility, the reduction of compound lotteries axiom states that χ_t and $\pi_{m,t}$ can be reduced to a single distribution, i.e. the social planner is uncertainty neutral. The social planner's welfare at time t writes recursively:

$$\begin{aligned} U_t(x_t, \epsilon_t) = \max_{y_t} \ & \left[u(x_t, y_t) + \delta \mathbb{E}_{\chi_t, \pi_{m,t}}(\tilde{U}_{t+1}(x_{t+1}, \tilde{\epsilon}_{t+1}))\right] \\ & s.t\ x_{t+1} = G(x_t, y_{t+1}) \text{ and } \mu_t \in \Gamma(x_t) \end{aligned} \tag{1}$$

with G the transfer function, $\tilde{U}_{t+1}$ the random continuation value, $\tilde{\epsilon}$ the stochastic component, δ the discount factor and u the instantaneous utility, assumed to be of the constant-relative risk aversion form with η the elasticity of marginal utility: $u(x) = \frac{x^{1-\eta}}{1-\eta}$.

This expected utility approach has two drawbacks. On the one hand, preference over time and states of the world are entangled in η. On the other hand, the social planner is uncertainty neutral: that may not be the most natural approach to decision-making under uncertainty (Ellsberg, 1961). Recent empirical evidences suggest that policy-makers are uncertainty-averse (Berger and Bosetti, 2020). For robustness, we test how much our estimates for optimal global climate policy and optimal regional subsystem management derived under expected utility depend on our collective attitude towards risk and uncertainty. Thus, our second recursive criterion is a specific form of smooth ambiguity criterion that allows to introduce uncertainty aversion from the social planner and to disentangle intertemporal elasticity of substitution and relative risk aversion. Among other social choice criteria used to study risk and uncertainty, we use a form of recursive smooth ambiguity model for three reasons. First, these preferences are an extension of the expected utility model which makes the comparison with

this framework more readable: as in this model, the flaw is that we have to define subjective probabilities for the different models. We assume that each model has an equal probability of being the 'right' one. The second reason is that this criterion allows a separation between the object (risk and uncertainty) from our attitude towards it (risk and uncertainty aversions). Thus, comparative statics with varying (risk) uncertainty aversion and constant (risk) uncertainty levels can be undertaken, whereas it is entangled in the penalty parameter in robust control (Hansen and Sargent, 2001). It is useful as our setting includes both risk and uncertainty. The third reason is that, in comparison with robust control, this model does not assume that the decision-maker has an approximate model and that the 'real' model is near this approximation.

Smooth-ambiguity With this criterion, χ_t and $\pi_{m,t}$ cannot be reduced to a single distribution (Hayashi and Miao, 2011; Berger et al., 2017). This is the case here when the concave transformation $h \circ v^{-1}$ introduced below is non-linear, yielding uncertainty aversion. Social planner's welfare at time t writes:

$$\begin{aligned} V_t(x_t, \epsilon_t) &= W(u_t, u(R_t(\tilde{V}_{t+1}(x_{t+1}, \tilde{\epsilon}_{t+1})))) \\ W(u, y) &= u^{-1}[(1-\delta)u + \delta y] \\ R_t(V_{t+1}(x_{t+1}, \epsilon_{t+1})) &= h^{-1}\left[\mathbb{E}_{\chi_t}\left(h \circ v^{-1}\mathbb{E}_{\pi_{m,t}}[v(\tilde{V}_{t+1}(x_{t+1}, \tilde{\epsilon}_{t+1}))]\right)\right] \end{aligned} \tag{2}$$

under the same constraints. W: $\mathbb{R}^2 \to \mathbb{R}$ is a time aggregator and R is an uncertainty aggregator that maps an ω_{t+1}-measurable random variable $\tilde{\epsilon}_{t+1}$ to an ω_t-measurable random variable. $\mathbb{E}_{\chi_t}$ is the expectation operator taken at time t over models, and $\mathbb{E}_{\pi_{m,t}}$ is the expectation operator taken at time t over future welfare, conditional on the model m. The three functions u, v and w are isoelastic, with θ, γ and μ the inverse of the elasticity of intertemporal substitution, the relative risk aversion and the relative uncertainty aversion. The two expectations highlight the two-step bayesian approach. In the first stage, the social planner evaluates the expected reward of a policy under each risky model and express it in monetary terms through a certainty equivalent that depends on her attitude towards risk. In the second stage, the policy maker evaluates an overall expected reward across the various certainty equivalents depending on her attitude towards uncertainty. The policy maker adresses risk within models, then uncertainty over models.

1.3 Analytical definitions

1.3.1 Global scale - optimal climate policy (SCC & SCCDS)

In the remainder of this work, SCC (SCC^{SA}) is the social cost of carbon under expected utility (smooth ambiguity), SCCDS (SCC) is the social cost of carbon when the dynamic subsystem is (not) included in the model. Without loss of generality, consider the optimal SCC and SCCDS for a policymaker under expected utility. For exposition, we focus on expected utility to highlight the various channels through which the subsystem affects optimal policy: same elements are derived under smooth ambiguity in annex. We simplify the notation for the expectation taken over stochastic risk and over models, reduced by compound lotteries under expected utility. The shadow cost of emissions is the negative partial derivative of the right-hand side of equation (1) with respect to time t emissions, S_t. It is brought from intertemporal utility to present monetary terms when scaled by the marginal utility of consumption $u_c'(c_t)$ and a discount factor δ. We assume no decay, so that $\frac{\partial S_{t+1}}{\partial S_t} = \frac{\partial T_{t+1}}{\partial T_t} = 1$. In our setting, we have stochastic aggregate risk over transient response to cumulative emissions, $\partial T/\partial S$, and idiosyncratic risk over the subsystem's dynamics, $\partial A/\partial T$. We assume that the impact of the subsystem on global temperatures goes through carbon releases rather than other mechanisms as in our quantitative application. SCC and SCCDS write:

$$SCC_t = \frac{\delta}{u_c'(c_t)} \mathbb{E}_t \left(\frac{\partial U_{t+1}}{\partial T_{t+1}} \frac{\partial T_{t+1}}{\partial S_{t+1}} \right) \tag{3}$$

$$\begin{cases} SCCDS_t = \frac{\delta}{u_c'(c_t)} \left[\underbrace{\mathbb{E}_t \left[\frac{\partial U_{t+1}}{\partial T_{t+1}} \frac{\partial T_{t+1}}{\partial S_{t+1}} \left(1 + \frac{\partial S_{t+1}}{\partial A_{t+1}} \frac{\partial A_{t+1}}{\partial S_t} \right) \right]}_{V_{1,t}\,:\,temperature\ channel} + \underbrace{\mathbb{E}_t \left[\frac{\partial U_{t+1}}{\partial A_{t+1}} \frac{\partial A_{t+1}}{\partial S_t} \right]}_{V_{2,t}\,:\,subsystem\ channel} \right] \\ V_{1,t} = \underbrace{\mathbb{E}_t \left(\frac{\partial U_{t+1}}{\partial T_{t+1}} \frac{\partial T_{t+1}}{\partial S_{t+1}} \right)}_{V_{1,t}^a\,:\,standard} \underbrace{\mathbb{E}_t \left(1 + \frac{\partial S_{t+1}}{\partial A_{t+1}} \frac{\partial A_{t+1}}{\partial S_t} \right)}_{V_{1,t}^b\,:\,subsystem\ scaling} + \underbrace{cov \left(\frac{\partial U_{t+1}}{\partial T_{t+1}} \frac{\partial T_{t+1}}{\partial S_{t+1}}; 1 + \frac{\partial S_{t+1}}{\partial A_{t+1}} \frac{\partial A_{t+1}}{\partial S_t} \right)}_{V_{1,t}^c\,:\,insurance} \end{cases} \tag{4}$$

Modeling an endogenous subsystem in a global climate-economy model and its interaction with climate change implies a risk premium that can be decomposed in two immediate channels: a subsystem channel and a temperature channel. First, marginal changes in the subsystem's state, affected by current marginal carbon emissions, have an impact on the continuation value: it is the subsystem channel. Second, a marginal increase in carbon emissions affect next period temperatures and fu-

ture welfare, both through the global carbon cycle and with the additional feedback on temperature from the subsystem: it is the temperature channel. The temperature channel has three components: a change in the continuation value of the standard channel driving optimal policy, a scaling factor of this same standard channel and an insurance component, the 'subsystem beta'.

The standard channel driving optimal climate policy, $\frac{\partial U_{t+1}}{\partial T_{t+1}} \frac{\partial T_{t+1}}{\partial S_{t+1}}$, is modified when we account for the subsystem's dynamics. In particular, $\partial U_{t+1}/\partial T_{t+1}$ can be decomposed in two components through a second-order taylor expansion depicted in annex: the certainty equivalent (CE) and the precautionary channel (PC), following Lemoine and Rudik (2017) and Lemoine (2021). Most of the future impacts on intertemporal welfare of a marginal carbon emission are included in the continuation value U_{t+1}. We decompose these impacts further for all future periods. Detailed in annex, the decomposition yields an expression for SCC and SCCDS:

$$SCC_t = \frac{\delta}{u'_c(c_t)} \overbrace{\sum_{i=t}^{\infty} \delta^{i-t} \, \mathbb{E}_t \left[u'_S(c_{i+1}) \right]}^{Complete\ standard} \tag{5}$$

$$SCCDS_t = \frac{\delta}{u'_c(c_t)} \left[\overbrace{\sum_{i=t}^{\infty} \delta^{i-t} \, \mathbb{E}_i \left(u'_S(c_{i+1}) \right) \, \Pi_{l=t}^{i} V_{1,l}^{b}}^{Complete\ standard\ channel\ scaled} + \overbrace{V_{1,t}^{c} + \sum_{j=t}^{\infty} \delta^{j-t+1} \, V_{1,j+1}^{c} \, \Pi_{m=t}^{j} V_{1,m}^{b}}^{Complete\ insurance\ channel} + \overbrace{V_{2,t} + \sum_{k=t}^{\infty} \delta^{k-t+1} \, V_{2,k+1} \, \Pi_{n=t}^{k} V_{1,n}^{b}}^{Complete\ subsystem\ channel} \right] \tag{6}$$

Modeling an endogenous subsystem in a global climate-economy model and its interaction with climate change implies a risk premium that can be decomposed in three complete channels, accounting for present and future impacts. The first term of equation (6) is the sum of all future marginal impact of an increase in the carbon stock on instantaneous utility. The second term is the complete insurance channel. The last term is the subsystem channel at all future periods. I describe the three scaled channels in detail below. The three channels driving optimal policy are scaled by all present and future $V_{1,i}^{b}$ when the subsystem's dynamics is explicitely accounted for. $V_{1,i}^{b}$ measures the sign and magnitude of the additional present and future feedbacks the subsystem brings to climate change. It increases (decreases) the SCCDS if $(\partial S_{i+1}/\partial A_{i+1}).(\partial A_{i+1}/\partial S_i)$ is positive (negative), i.e. if the subsystem releases (absorbs) carbon when carbon concentration increases.

Complete standard channel scaled The first term in the bracket in equation (6) is the complete standard channel scaled. Introducing a climate subsystem in a dynamic climate-economy model scales the standard channel driving optimal climate policy by the present and future expected feed-

backs this subsystem brings on climate change, and thus on intertemporal welfare through climate damages. The standard channel driving optimal climate policy is the sum on all present and future period of the marginal derivative of instantaneous utility with respect to a marginal increase in carbon concentration.

Complete insurance channel The second term in the the bracket in equation (6) is the complete insurance channel. This insurance channel measures how the additional feedback on climate change brought by the impact of climate change on the subsystem's dynamics covaries with the marginal impact of carbon emissions from economic activity on intertemporal welfare at all present and future period. This term V_1^c is familiar from the consumption-based capital asset pricing approach (Lucas Jr, 1978) and the climate-economics literature (e.g. Dietz et al. (2018), Lemoine (2021), Van den Bremer and Van der Ploeg (2021)): agents require a greater expected return on assets which increase aggregate risk bearing on future consumption[1]. The left-hand side of this channel is the marginal effect of a change in cumulative emissions on intertemporal welfare: it is negative. The right-hand side of the covariance can be either positive if the marginal impact of a change in carbon concentration[2] on subsystem's state has the same sign as the marginal impact of a change in subsystem's state on carbon concentration, or negative if they have opposite signs. All these states of the world are possible within the same model and for the same dynamic subsystem. In the first case, the feedback of the subsystem on climate change is positive: a marginal increase in carbon concentration brings an even larger temperature change because of the change in subsystem's dynamics. The causal mechanism stems either from a growth effect (an increase in carbon concentration increases the subsystem's state which increases the temperature) or a degrowth effect (an increase in carbon concentration decreases the subsystem's state which decreases temperature). Examples of subsystem that have these cyclical properties are for instance cryosphere climate tipping elements (Armstrong McKay et al., 2022), such as the boreal permafrost, and the Greenland, West and East Antarctic ice sheets. In the second case, the feedback of the subsystem on climate change is negative: the effect of a marginal increase

[1] A parallel beta could be computed for scientific uncertainty, measuring how scientific uncertainty about this subsystem's dynamics and its interaction with climate change affects aggregate scientific uncertainty about climate change. A positive beta-risk, i.e. when the subsystem increases aggregate risk, should be decreased (increased) if the subsystem's uncertainty decreases (increases) aggregate scientific uncertainty, i.e. depending on subsystem beta-uncertainty (Izhakian, 2020).

[2] In our analytical decomposition, we focus on temperature impacts through the carbon cycle, but the demonstration would apply to other mechanisms.

in temperature on temperature is mitigated by the decrease in temperature from the subsystem. Two causal mechanisms are possible: either a growth effect (an increase in carbon concentration increases the state of the subsystem which decreases the temperature) or a degrowth effect (an increase in temperature decreases the subsystem which increases the temperature). Examples of subsystem that have these countercyclical properties are for instance ocean-atmosphere climate tipping elements, such as Labrador-Irminger Seas, Subpolar Gyre (SPG) oceanic Convection and Altantic Meridional Overturning Circulation (AMOC). If the feedback brought by the subsystem covariates positively (negatively) with the impact of emissions on intertemporal welfare, then optimal policy is relatively more (less) stringent when this 'subsystem beta' is accounted for. The magnitude of the covariance depends on relative variations: for a positive covariance, if the states of the world where the marginal effect of an additional emission on welfare is relatively greater (smaller) are also the states of the world where the right-hand side of the covariance is relatively greater (smaller), i.e. situation where the feedback of the subsystem on climate change is relatively more positive (more negative), then the insurance channel increases the social cost of carbon SCCDS more (less). This depends on subsystem dynamics, global climate damage, global temperatures, etc.

Complete subsystem channel The third term in the the bracket in equation (6) is the complete subsystem channel, i.e. the sum of all present and future immediate subsystem channels $V_{2,t}$ scaled by the feedback of the climate subsystem on global climate change. The complete subsystem channel measures how a marginal change in the subsystem's state due to a marginal carbon emission affects intertemporal welfare. A contemporary increase in carbon concentration and in temperature has a stochastic impact on the subsystem. This impact can be sometimes positive, for instance if an increase in carbon concentration increases vegetation growth rates for rainforests because of fertilization effects. But the impact of a marginal emission is mostly negative, as increases in carbon concentration disrupts most climate subsystems (Armstrong McKay et al., 2022), such as the Barents Sea Ice. This impact can also be alternatively positive or negative for a given subsystem depending on its own dynamics or the current state of the climate system. A same marginal increase in carbon concentration does not have the same impact along a given concentration pathway. For instance, a marginal increase in carbon concentration at low concentration levels might increase the vegetation growth rate for the Amazon rainforest through fertilization effects, while an increase in carbon concentration at high concentration levels might put the rainforest in great danger through changes in El Niño, a collapse in the Atlantic meridional overturning circulation or temperature limits for the

photosynthesis (Doughty et al., 2023). A same marginal increase in carbon concentration does not have the same impact depending on the state of the subsystem. For instance, while the Amazon rainforest might be resilient when not too disturbed, because of plant trait diversity (Sakschewski et al., 2016) or evapotranspiration by which the rainforest recycles the rainfall that will feed its future growth, these characteristics that enhance resilience of the subsystem might weaken when the subsystem's state decreases in extent. All these characteristics of the impacts a climate subsystem might have on intertemporal welfare are disregarded when the subsystem is not explicitely a state variable of our program and its collapse represented as an *ad hoc* probability depending on carbon concentration.

Including a subsystem in a global climate-economy model and its interaction with global climate change implies a risk premium that can be decomposed in three components: a scaling of standard optimal policy measure, an insurance component, and a subsystem component. Each of these channels is scaled by the additional feedback the subsystem brings on global climate change in all present and future periods.

1.3.2 Regional scale - optimal subsystem's management (SCDS)

The social cost of the dynamic subsystem, SCDS, is the marginal impact on intertemporal welfare of a marginal change in subsystem's state, brought into present monetary terms. In other words, a marginal change in the current state of the subsystem has an impact on the future dynamics of the subsystem, which matters because this future dynamics has an impact on future climate damages. The subsystem has its own dynamics, which is not completely controlled by the policy-maker. Our representation of the dynamics of the subsystem allows to highlight and compute the SCDS. Without loss of generality, we derive the SCDS under expected utility. The same formula is given in annex for smooth ambiguity.

Starting from the optimal policy program, we seek for the derivative of our continuation value with respect to the subsystem's state. In comparison with SCCDS, we focus on the marginal derivative of the next-period continuation value with respect to next-period subsystem's state. Indeed, the subsystem might have short-term oscillatory behavior: thus, $\partial A_{t+1}/\partial A_t$ might have unstable varying signs. Under moderate conditions, for instance along the optimal path, reducing the subsystem's stock could increase its short-term growth by for instance reducing competition between patches of a forest, while still reducing its aggregate long-term survival that is of interest to public policy. A short-term oscillation $\partial A_{t+1}/\partial A_t < 0$ might thus bias the sign of the SCDS while we are interested

in the long-term behavior of our system, i.e. its marginal impact on aggregate intertemporal welfare. $\mathcal{L}$ is the initial value of the carbon stored in the subsystem in our application ; this rescaling allows to translate marginal changes in the subsystem's state to a standard carbon unit. The SCDS has two different components:

$$SCDS_t = \frac{1}{\mathcal{L}} \frac{\delta}{u_c'(c_t)} \left[\underbrace{\mathbb{E}_t \left(\frac{\partial U_{t+1}}{\partial T_{t+1}} \frac{\partial T_{t+1}}{\partial S_{t+1}} \frac{\partial S_{t+1}}{\partial A_{t+1}} \right)}_{W_{1,t} : \textit{temperature channel}} + \underbrace{\mathbb{E}_t \left(\frac{\partial U_{t+1}}{\partial A_{t+1}} \right)}_{W_{2,t} : \textit{subsystem channel}} \right] \tag{7}$$

The temperature channel measures the feedback of the subsystem on aggregate climate change, i.e. how much a marginal change in the subsystem's state affects intertemporal welfare through its marginal impact on temperatures. The subsystem channel measures how a marginal change in the subsystem's state affects intertemporal welfare: it includes all future risk on the dynamics of the subsystem brought by a marginal perturbation in its current state, and thus all future potential increases in aggregate temperatures and climate damages, including the most disastrous.

We have highlighted the channels through which our modelling approach affects global climate policy and regional subsystem management. For illustration, we apply our framework to the debated fate of the Amazon rainforest. We quantify the impact of this specific subsystem on optimal climate policy in a dynamic stochastic climate-economy model. We measure the impact of the interactions between aggregate climate risk and amazon idiosyncratic risk and its explicit geophysical dynamics on optimal rainforest management. We compute the share of each of the channels depicted analytically.

2 A quantitative application: the Amazon rainforest

We use a macroeconomic growth model *à la Ramsey* and add climate dynamics (Guivarch and Pottier, 2018; Taconet et al., 2021; Fillon et al., 2023). We augment the model with a stylized representation of the Amazon rainforest whose uncertain dynamics interacts with climate change. We focus on two sources of stochasticity[3] that are of particular interest: standard aggregate climate risk regarding transient climate response to cumulative emissions on the one hand, i.e. how much emissions from economic activity translates to climate change, idiosyncratic stochastic impact of global

[3]More stochasticity and states would be difficult to handle with global solution methods without message passing interface on large computing clusters and would not provide more information on the mechanisms we want to highlight.

climate change on forest dynamics on the other hand, i.e. how much climate change affects the carbon stored in the rainforest. In other words, we price the Amazon rainforest climate asset within a broader risky climate portfolio. In addition to this stochasticity, we add an explicit geophysical representation of forest dynamics. The dynamics of the rainforest is self-sustaining, with possible feedback effects: a decrease in the forest cover decreases forest growth. This non-linear dynamics can generate some curvature in our value function in one dimension of our program. We include scientific uncertainty over both the functional form of this dynamics and on the impact of climate change on the rainforest, i.e. alternative scientific models embedded in our social choice. We identify key mechanisms and channels through which risks and uncertainties about the impact of global climate change on the rainforest affect optimal climate policy at the global scale and optimal rainforest management at the regional scale. We solve our recursive programs using dynamic programming: we interpolate recursively starting from the last period terminal value function and approximate our value functions with simplicial Chebyshev polynomials and adaptive approximation domains for our state variables (Cai, 2019). We employ simplicial Chebyshev polynomials, as they enable varying degrees of approximation across different dimensions of our dynamic problem: less precision is required for approximating the smooth dynamics of capital accumulation compared to the more complex dynamics of the Amazon rainforest. We break one level of 'curse-of-dimensionality' related to approximation nodes with parallel CPU computing for value function interpolation. Once we have interpolated recursively at each time step, we simulate 100 stochastic paths for each specification and use the mean path for each variable of interest.

2.1 Model specification

Economic model One global region produces at each period t a single good using capital K and exogenous labour L through a production function $F(K, L)$, with exogenous Hicks-neutral technological change from Nordhaus (2018). Capital dynamics is determined by the per-period capital depreciation δ and savings rate s: $K_{t+1} - K_t = -\delta K_t + Y_t s_t$. We assume a fixed savings rate $s_t = \alpha\delta$, where α is the share of capital in the Cobb-Douglas production function and δ the discount factor. Gross output $\bar{Y}$ is affected by a damage factor that increases with global average temperature T. Net output Y is derived from gross output net of damage: $Y = \Omega(T)F(K, L)$. Net output induces emissions, which can be mitigated at a certain cost: $E = \sigma Y(1 - \mu)$ with μ the abatement rate and σ the carbon content of production that decreases exogenously over time (Nordhaus, 2018). The emissions adds

up to a global cumulative emissions stock S and we assume no decay. The social planner trades off consumption and mitigation to maximize intertemporal welfare.

Climate model We use a simple representation for the climate system, with a linear formula linking global temperature T to the stock of global carbon emissions S through transient climate response to cumulative carbon emissions ψ, i.e. $\partial T/\partial S = \psi$, as in Dietz and Venmans (2019). Following Barnett et al. (2020), we assume a truncated normal distribution for ψ on the support $[0:3.5]$ with a best estimate of $\bar{\psi}$=1.73°C per 1000PgC and a standard deviation of 0.493. Quadratic climate damage to economic output Ω are derived from this change in average temperature.

Amazon rainforest The variable A used to represent rainforest's dynamics is the ratio of current carbon stored in the forest in comparison with the total possible carbon losses $\mathcal{L} = 75$GtC (Armstrong McKay et al., 2022). We use a stylized vegetation dynamics (Ritchie et al., 2021), where the dynamics of A is a function of the current state A and of regional temperature T_{reg} interacted with the stochastic impact of climate on tree mortality via droughts $\tilde{\epsilon}$. T_{reg} is deduced from global cumulative emissions stock via linear and time-invariant regional transient climate response to global cumulative emissions (Leduc et al., 2016). There are two possible functional forms for the dynamics of the system: either without (f_1) or with (f_2) a feedback effect. There are four distributions for $\tilde{\epsilon_j}$ because four different climate models j are used to estimate how more frequent and intense droughts are under changing climate. This yields a total of eight models: we give each model m the same probability of being the 'true' one. The Lotka Volterra equation writes:

$$\frac{dA_{ij}}{dt} = \begin{cases} f_i(\tilde{\epsilon_j}.T_{reg}, A_{ij}) \text{ with } i \in \{1,2\}, j \in [1:4] \text{ if } t \leq 2200 \\ 0 \text{ if } t > 2200 \end{cases} \tag{8}$$

$$\text{with} \begin{cases} f_1(x) = g_0 \left[1 - \left(\frac{T_{reg}(0)+T_{reg}}{\beta_0}\right)^2\right] x(1-x) - \tilde{\epsilon_j} T_{reg} x - \kappa x \\ f_2(x) = g_0 \left[1 - \left(\frac{\Upsilon[1-x]+T_{reg}(0)+T_{reg})}{\beta_0}\right)^2\right] x(1-x) - \tilde{\epsilon_j} T_{reg} x - \kappa x \end{cases} \tag{9}$$

where g_0 is the forest growth rate under normal conditions, κ exogenous deforestation and degradation rates, $T_{reg}(0)$ regional temperature increase with respect to preindustrial at initial time, T_{reg} regional temperature increase with respect to initial time, β_0 half-width of the growth versus temperature curve, and Υ the temperature difference between bare soil and forest, driving the feedback. We assume that regional transient climate response to global cumulative emissions, from which T_{reg} is

deduced, does not depend on A, which should hold for any optimal policy path where the rainforest is not too depleted.

2.2 Calibration

We use a standard calibration for the climate and macroeconomic modules: a complete description is given in annex. We use exogenous deforestation and degradation scenarios. Our calibration is a two-step procedure. We first calibrate the maximum impact of climate on the rainforest via droughts using climate model projections and historical observations. Then, given these parameters, we jointly calibrate the remaining parameters internally so that the probability of forest dieback under a tipping risk (i.e. with functional form f_2 that includes a feedback effect in the dynamics) matches the central estimate of the core expert probability assessment of Kriegler et al. (2009) for each of their temperature corridors. In particular, we calibrate the shape of the distribution of $\tilde{\epsilon}$ between 0 and its estimated upper bound. We then assume that the parameters and the distribution for $\tilde{\epsilon}$ remains constant for the other specification f_1 where there is no tipping risk.

Exogenous deforestation and degradation κ At each period t, a share κ_t of the current forest cover is deforested or degraded. We use the mean of three deforestation scenarii (Aguiar et al., 2016). We assume that deforestation stops after 2050 as this is the maximum horizon for most scenarios. We multiply the area deforested by two to take into account forest degradation, including human-induced fires, based on the historical relationship observed between deforestation and degradation (Matricardi et al., 2020). Scenarii are for the brazilian Amazon which covers 60% of the extent of the rainforest: we scale the scenario and assume that they hold for the whole rainforest. We convert the deforestation rate expressed in km^2 in a share of initial carbon storage, assuming homogeneity of the carbon stored over the forest.

External calibration - Endogenous climate change effects $\tilde{\epsilon}_j$ via droughts We model this link through four $\tilde{\epsilon}_j$ based on the climate model j used to predict the change in rainfall patterns. We assume that each $\tilde{\epsilon}_j$ follows a Beta distribution on a support whose upper limit $\bar{\epsilon}_j$ is estimated below. For the estimation of these upper bounds, we exploit in each climate model the variation in local climate conditions to measure how much carbon losses from tree mortality in the Amazon increases with local temperatures. A complete description of our econometric study can be found in the annex.

We build a balanced panel dataset until 2100 along three representative concentration pathways (RCP 2.6, 6.0, 8.5) and use 60 arc-minutes resolution gridded data from the Inter-Sectoral Impact Model Intercomparison Project (ISIMIP) on monthly precipitation. We use precipitation projections taken from the hydrological model MATSIRO for all possible climate forcing models *j*: IPSL-CM5A-LR, HadGEM2-ES, GFDL-ESM2M, MIROC5. We compute an index of precipitation stress, the yearly maximum cumulative water deficit (MCWD) anomaly with respect to an historical baseline (1985-2004). We match this precipitation data with bias-adjusted and downscaled gridded surface temperature data specific to each climate forcing model. Data from historical observations (Phillips et al., 2009; Yao et al., 2022) established a link between MCWD anomaly and carbon losses from tree mortality in the Amazon rainforest. We scale these yearly carbon losses obtained for each climate forcing model by the spatial heterogeneity observed in the carbon storage at initial time, taking data from EarthData (NASA). Our preferred specification is a fixed-effect approach with year and regional fixed effects and Driscoll and Kraay (1998) standard errors to account for heteroskedascicity and serial correlation. We control for sub-regional diversity with Silva-Souza and Souza (2020) woody plant regionalization into 13 subregions. The dependent variable is the yearly carbon loss from tree mortality (in tC/ha/y) at the cell level for each climate model, and the independent variable is the local temperature observed over the same period (in °C). We estimate the following equation:

$$C^{j}_{i,r,t} = \beta^{j}_{carbon} X^{j}_{i,r,t} + \alpha^{j}_{i} + \delta^{j}_{t} + \zeta^{j}_{r} + \iota^{j}_{i,r,t} \tag{10}$$

with u the pixel-specific error term, i the grid cell, t the time period, r the Silva-Souza and Souza (2020) subregions. β^{j}_{carbon} is our coefficient of interest, α a vector of N-1 location-specific fixed effect and the constant, δ a vector of time fixed effects and ζ our vector of region-specific fixed effects to account for clusters in our data. We obtain our coefficient of interest $\hat{\beta}^{j}_{carbon}$ for four climate models. We multiply $\hat{\beta}^{j}_{carbon}$ by the size of the rainforest, $\approx$ 700 million ha (Silva-Souza and Souza, 2020), to obtain the yearly loss of carbon per additional degree of local temperature for each model j. We express this coefficient as a share of the total initial carbon stored that could be released under total dieback (75 GtC) and multiply by the number of years per period to obtain the maximum share of carbon stored in the rainforest that is lost per period because of droughts for a one degree increase in local temperature for each model j, $\bar{\epsilon}_{j} \in \{0.0376, 0.0661, 0.0774, 0.1447\}$. Our dynamic model relies on regional temperature that depends linearly on the cumulative global emission stock (Leduc et al., 2016): we make the assumption that the link between carbon losses and local temperatures holds for regional temperatures.

Internal calibration Information on how to evaluate the probability of a tipping point for the Amazon is scarce. We use expert's elicitations of a possible Amazon tipping point depending on temperature corridors expressed in Kriegler et al. (2009). $\tilde{\epsilon}$ is the coefficient and its probability distribution is a mixture of the four ϵ_j. $\tilde{\epsilon}$ follows a Beta law with parameter α_s and β_s over the support $[0 : \bar{\epsilon}]$ where $\bar{\epsilon}$ is the mean of the maximum $\bar{\epsilon_j}$. We jointly calibrate Υ, g_0, α_s, β_s so that the probability of tipping, dependent on the distribution of $\tilde{\epsilon}$, follows approximately the central probability of the expert assessments. We have that $g_0 = 0.49$, $\Upsilon = 6$ and $\tilde{\epsilon} \sim$ B (0.36,0.32) with support $[0 : \bar{\epsilon}]$. For illustration, we simulate the cumulative carbon losses for all SSP under our model[4].

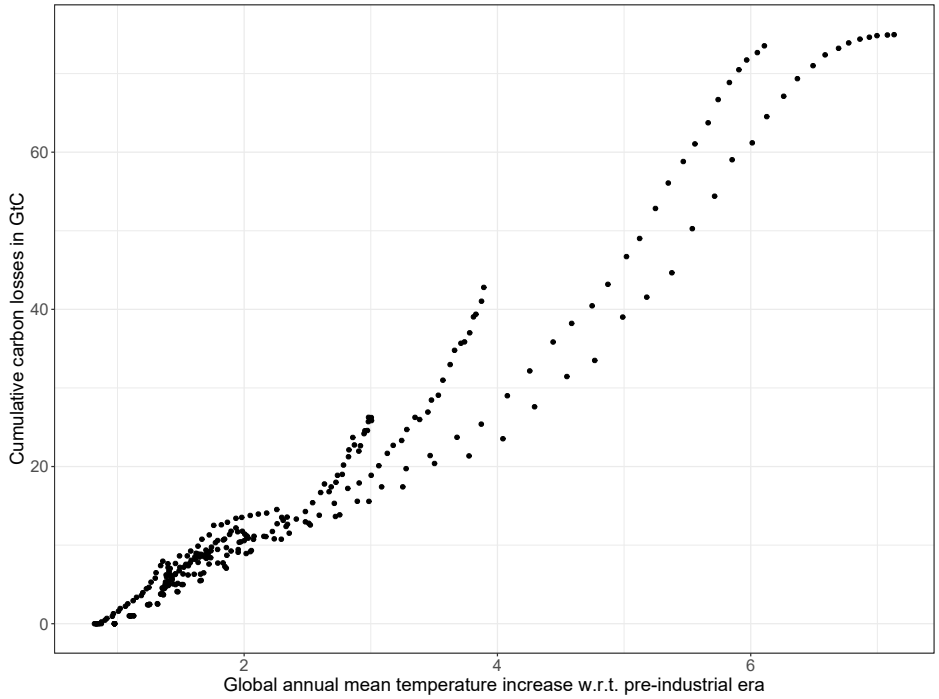

Figure 1: Mean net cumulative carbon losses (in GtC) from the Amazon rainforest along mean temperature increases with respect to preindustrial era from various extended concentration pathways (SSP1-1.9, SSP1-2.6, SSP4-3.4, SSP5-3.4, SSP2-4.5, SSP4-6.0, SSP3-7.0, SSP5-8.5), from 2000 to 2200, under our calibration.

A partial or total dieback of the forest occurs by 2200 for a temperature increase with respect to pre-industrial era above 4°C, which is well above temperature levels obtained under optimized paths.

[4]In appendix, we plot phase diagrams of the stochastic dynamic system in Figures (8) and (9) for the whole distribution of ϵ and different temperature pathways over time.

Thus, while our calibration is approximate, the dynamics of the forest in our estimate is not artificially more catastrophic to inflate policy estimates.

2.3 Results

We assess numerically the optimal climate policy in a stochastic model with an explicit modelling of the Amazon's dynamics under risk and uncertainty. We first measure how much the social cost of carbon at the global scale is affected by the Amazon rainforest under expected utility. In other words, we study the gap between SCC and SCCDS. We quantify how the various channels depicted above shape optimal global climate policy. Second, we quantify the social cost of the dynamic subsystem SCDS as a share of the standard social cost of carbon SCC under expected utility. Finally, for robustness, we price the risks and scientific uncertainties in the Amazon dynamics and its interaction with global climate change and the macroeconomy under smooth ambiguity: we quantify SCC^{SA} and SCCDS^{SA} under various specifications. In annex, we present intertemporal stochastic paths for our control variable and for two state variables of interest: global average temperature and amazon rainforest's state with respect to its initial state.

2.3.1 Optimal global climate policy - SCC and SCCDS

We first compute SCCDS under expected utility. We compare SCCDS to the standard SCC that would be obtained under stochastic aggregate climate risk but without an explicit endogenous modeling of the Amazon rainforest. On Figure (2), we plot the increase (in %) from SCC to SCCDS for two specifications. The left bar shows the increase the Amazon rainforest brings to the SCC at the global scale when there is climate risk on the transient climate response to cumulative emissions but no idiosyncratic risk over the rainforest dynamics. The right bar shows the increase from SCC to SCCDS when we include both idiosyncratic stochastic risk in the dynamics of the rainforest and aggregate climate risk. For each measure, we compute the share that each of the various channels identified in the complete analytical decomposition from equation (4) contributes to the increase from SCC to SCCDS: the scaling of the standard channel through which carbon emissions affect intertemporal welfare, the insurance 'amazon beta' component, and the subsystem channel by which a marginal change in the amazon's state affects intertemporal welfare through the continuation value.

Figure (2) yields two main results. First, including the endogenous dynamics of the Amazon rainforest in a dynamic stochastic climate-economy model increases the SCC. Under aggregate cli-

mate risk over the transient climate response to cumulative emissions, the SCCDS that includes the dynamics of the Amazon rainforest is around 11% larger than the standard SCC. When additional idiosyncratic risk on the dynamics of the rainforest is added, i.e. stochastic risk on the impact of stochastic drougts from climate change on the rainforest, the SCCDS is around 15% larger than the SCC. In their meta-analysis based on Cai et al. (2016), Dietz et al. (2021) highlight that the possible dieback of the Amazon rainforest leads to a 0.1% increase in the expected SCC when considering its value as a carbon stock. Our analysis suggests these estimates may be significantly understated for two reasons. First, we account for the rainforest's dynamics across all possible future states, rather than focusing on a stylized, catastrophic risk of partial dieback. Second, we incorporate the marginal impact of the rainforest subsystem on the continuation value—a mechanism described as the subsystem channel in equation (4). This channel is not explicitly captured in standard climate-economy models, which often rely on *ad hoc* probabilities for subsystem dieback without integrating an explicit state variable to represent the subsystem's dynamics.

Our second result from the right histogram on Figure (2) shows indeed that the largest share of the increase from SCC to SCCDS stems from the subsystem channel. Under climate risk, the subsystem channel represents around 74.3% of this increase, the scaling of the standard SCC by the additional feedback from carbon releases of the Amazon rainforest represents 25.3%, and the insurance channel represents 0.4%. Under both aggregate climate risk and idiosyncratic amazon risk, the subsystem channel accounts for 68%, the standard scaling represents 31.4%, and the insurance channel 0.6%. In other words, most of the increase between SCC and SCCDS stems from the subsystem channel under both specifications. The insurance channel, on the other hand, is rather weak, which can be explained by two factors. First, the risk specification in our model: the insurance relates to the interaction between the aggregate climate risk (transient climate response to cumulative emissions) and the idiosyncratic risk (of changing carbon concentration on forest dynamics). In reality, there are other sources of risk between the two systems, such as the risk on the forest impact on the climate system, i.e. stochasticity in possible carbon releases that might for instance arise due to heterogeneity over the rainforest in the carbon storage. This risk could increase the insurance component, i.e. the subsystem's contribution to the aggregate risk. Second, we study one subsystem in isolation, whereas there are several subsystems that interact with each other and could increase the overall aggregate risk, for example El Niño or AMOC and their feedbacks with the Amazon rainforest via precipitation cycles.

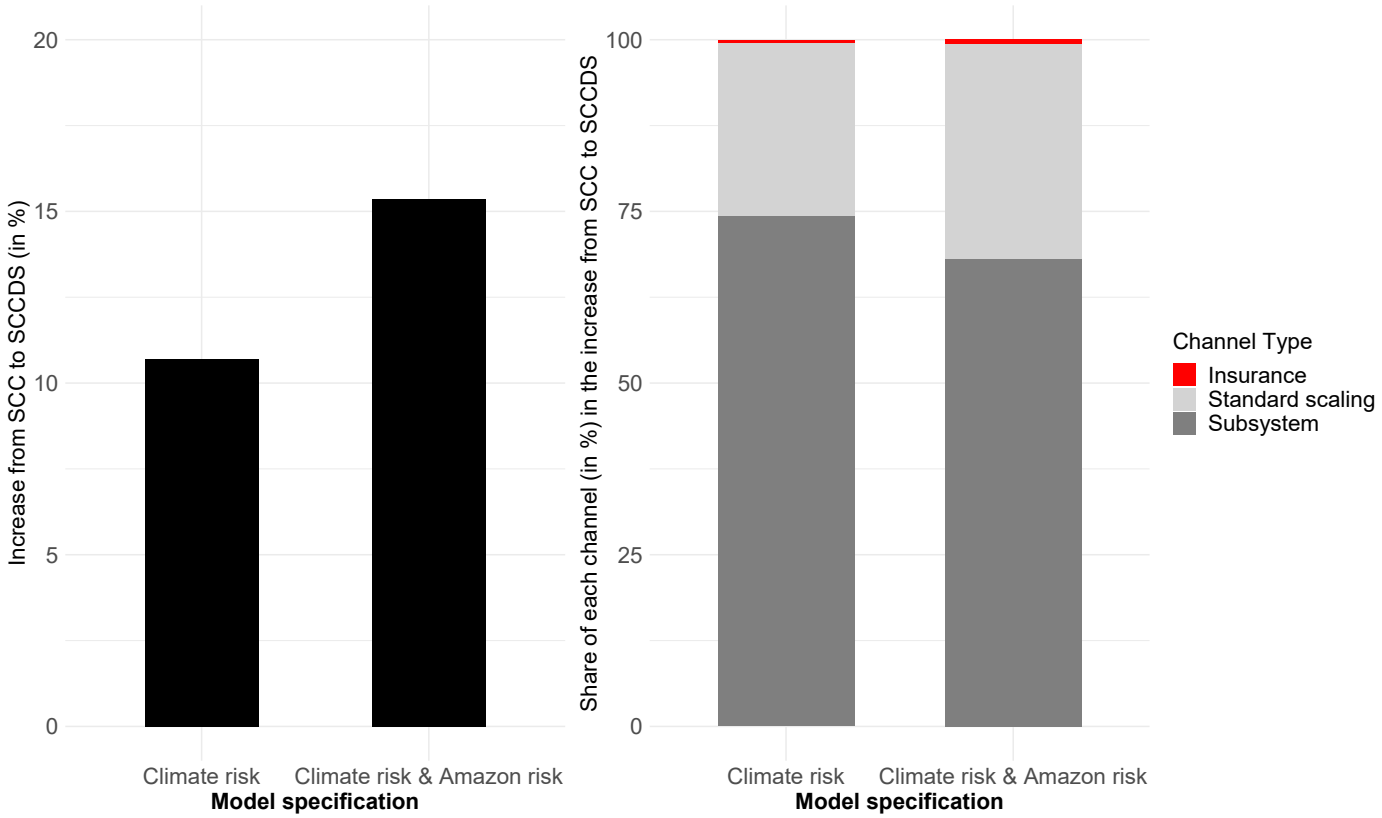

Figure 2: **Left** Increase (in %) from SCC to SCCDS when the Amazon rainforest is added to the dynamics system, under stochastic aggregate climate risk (left), under both stochastic aggregate climate risk and idiosyncratic amazon risk (right). **Right** Share (in %) of each channel in this increase (scaling, insurance & subsystem channels) under aggregate climate risk (left) and both aggregate climate and idiosyncratic amazon risks (right).

A back of the envelope calculation helps to understand the magnitude these percentages might represent. Using a 2% discount rate, U.S. Environmental Protection Agency recently suggested to use a \$190 per tCO_2 social cost of carbon (Agency, 2022). Global CO_2 emissions in 2022 are estimated at $36.4GtCO_2$ (Friedlingstein et al., 2023). This means that if the increase from SCC to SCCDS under both stochastic risks represents 15% of the standard SCC, applying this increase to the universe of CO_2 emissions would raise around 1.0374 trillion dollar for 2022 only. Even the insurance channel, which represents only 0.6% of these 15% increase, accounts for nearly 6 billions dollar yearly, i.e. five time the \$1.2 billion pledges from Lula da Silva for the Amazon Fund in January 2023. The wedge between SCC and SCCDS could be leveraged at the global scale to finance coasian mechanisms at the regional scale to prevent deforestation and forest degradation. This regional management

could indeed decrease the subsystem channel and reduce risk over the future dynamics of the Amazon rainforest. This global redistribution would have a double dividend property: it would reduce both the negative externality of carbon emissions at the global scale and the global and regional risk over the dynamics of the rainforest.

Explicitly introducing the dynamics of a climate subsystem such as the Amazon rainforest into stochastic climate-economy modelling has an impact on optimal global climate policy. To assess the value of a hectare of Amazonian forest focusing only on its use value as a carbon stock, we first need to quantify the amount of carbon stored in that hectare Σ. Once this quantity is known, it must be multiplied by the standard social cost of carbon. Then, it should be multiplied by the increase implied by the stochastic modeling of the dynamic of the subsystem estimated above, i.e. $\Sigma * SCC * 1.15 = \Sigma * SCCDS$. But that is not all. Explicitly introducing the dynamics of a climate subsystem such as the Amazon rainforest into stochastic climate-economy modelling also has an impact on the optimal management of the subsystem's resilience over time.

2.3.2 Optimal regional rainforest management - SCDS

We compute the social value of the dynamics system (SCDS) under expected utility as a share of standard social cost of carbon SCC under aggregate climate risk but without the amazon rainforest included in the dynamics, i.e. the standard measure of the SCC in the literature. On Figure (3), we plot the share for two specifications. On the left, we plot this share under standard aggregate climate risk. On the right, we plot the share under both standard aggregate climate risk and idiosyncratic amazon risk. For each specification, we report the share of the two channels analytically depicted in equation (7) in the SCDS.

Figure (3) yields two key results. First, SCDS represents a significant share of the SCC. Under aggregate climate risk, the SCDS represents 15.77% of the SCC. Under both aggregate climate risk and idiosyncratic risk over the dynamics of the rainforest, this share increases to 15.95%, a 1.1% increase with respect to the specification with aggregate climate risk only. Second, what matters most in the SCDS is the subsystem channel, i.e. the impact of a marginal change in the subsystem's state on the continuation value of our program, which includes all future risks over the dynamics of the forest and the welfare impacts of future possible carbon releases. Under aggregate climate risk, the subsystem channel represents 58.2% of the SCDS. Under both aggregate climate risk and

idiosyncratic subsystem risk, the subsystem channel represents 57.6% of the SCDS.

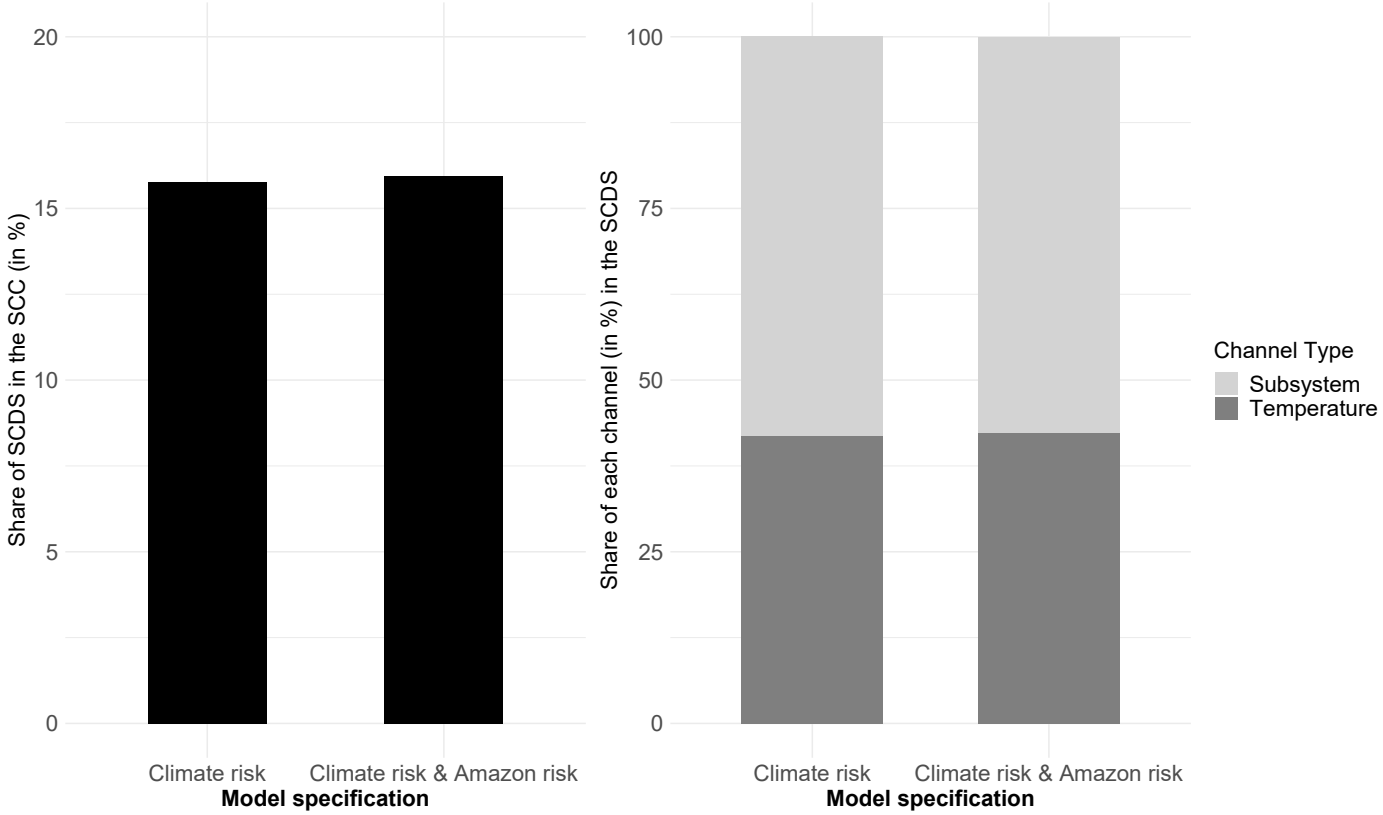

Figure 3: **Left** Share (in %) of SCDS in the SCC under expected utility with stochastic climate risk under deterministic and stochastic specifications for the rainforest, i.e. without (left) and with (right) idiosyncratic amazon risk. **Right** Share (in %) of each channel in the SCDS (temperature and subsystem channels) under aggregate climate risk (left) and both aggregate climate risk and idiosyncratic amazon risk (right).

This has large implications for regional forest management. Indeed, when evaluating the value of a marginal hectare of rainforest in regional cost-benefit analysis, for instance for infrastructure projects, SCDS should be accounted for. In addition to the direct value of the carbon contained in this hectare of forest, which should be valued at the SCCDS level as argued above, we need to take into account the marginal value of the dynamic system on the continuation value, i.e. the sub-system channel of the SCDS. Indeed, choosing to deforest in one place releases carbon, but also has an impact on the forest's future carbon release dynamics and the probability of its dieback. Explicitly introducing the dynamics of a climate subsystem such as the Amazon rainforest into stochastic climate-economy

modelling has an impact on optimal regional subsystem management via the valuation of an hectare of rainforest. To assess the value of a hectare of Amazonian forest focusing only on its use value as a carbon stock, we first need to quantify the amount of carbon stored in that hectare. Once this quantity Σ is known, it must be multiplied by the standard social cost of carbon. Then, it should be multiplied by the increase implied by the stochastic modeling of the dynamic of the subsystem estimated above, i.e. $\Sigma * SCC * 1.15$. Finally, it should be scaled by the impact of a marginal change in the subsystem's state on the future of the rainforest, i.e. $\Sigma * SCC * (1.15 + (0.1595 * 0.576)) = \Sigma * SCC * 1.24$, which means a 24% increase in the valuation of this hectare of rainforest with respect to a standard valuation using the stochastic SCC under standard aggregate climate risk without the explicit modelling of the rainforest.

Revolution in satellite data has allowed a quick development in dynamic discrete choice methods that are useful tools to evaluate counterfactual policies (Araujo et al., 2020). While this granularity in satellite data is very complementary to our approach and important from a descriptive point of view in order to compute carbon stocks at the finest resolution or to monitor human disturbances on the forest in real time, it does not allow for prospective modelling of the system's dynamics. Although some early warning signals of critical transitions such as tipping points have been identified (Scheffer et al., 2009), they are not yet sufficiently developed for real-time monitoring. Furthermore, it is not certain that it is not too late once these signals are readable as the tipping point might already have been triggered irreversibly: Biggs et al. (2009) suggest that research should focus on defining critical indicator levels rather than detecting change in the indicators. We are in line with this robust approach to possible ecological regime shifts and SCDS might be operationalized to work in this direction within a global welfarist framework.

2.3.3 Robust social choice

Finally, for robustness, we look at the extent to which our attitude towards the large risks and uncertainties over the future dynamics of the rainforest can change the amplitude of our results on the SCCDS and SCDS under expected utility. We disentangle preference over time, risk and uncertainty (θ, γ and μ) under perturbations to the rainforest. Various parameter values are used in the literature either with positive or normative approaches (Ju and Miao, 2012; Cai and Lontzek, 2019). Our

approach is close to Berger et al. (2017): we assume as a benchmark[5] a setting with low-aversion $\theta = 1.5$, $\gamma = 2$, $\mu = 2$. The sensitivity is done on a high-aversion scenario with $\gamma = 10$, $\mu = 10$ while holding preference for intertemporal substitution constant. Under robust control, switching attitudes from low to high aversions yields an increase of about 40% for the SCCDS^{SA} and 60% for the SCDS^{SA}.

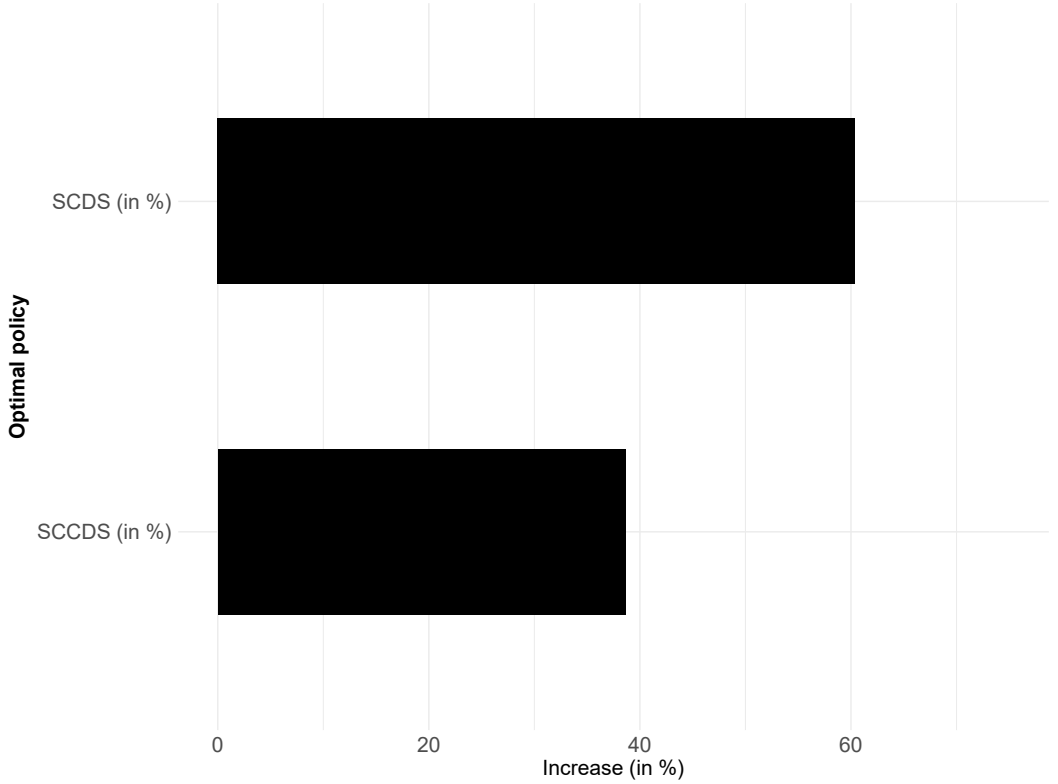

Figure 4: Increase (in %) from low to high risk aversion parameter values under smooth ambiguity when the amazon rainforest is accounted for (Top) SCDS^{SA} (Down) SCCDS^{SA}.

In our robust criterion, we abstract from learning as in Millner et al. (2013) and Berger et al. (2017). A dynamic learning model under uncertainty would require updating the weights given to each model. Even if is not clear how and in which direction scientific progress will allow to reduce uncertainty, our estimates under uncertainty aversion should be considered as upper bounds of the possible increases in the SCCDS brought by uncertainty. Meanwhile, a careful study of learning under a tipping risk (Rudik, 2020) shows that learning can backfire and reduce welfare by erroneously

[5]We cannot directly compare robust social choice policy programs to expected utility under risk has they do not yield the same deterministic paths.

ruling out pending catastrophe. Our upper bound ruling out learning could be more in line with a robust approach to decision-making under uncertainty.

Conclusion

Modeling stochastic and debated interactions between climate change, the macroeconomy and Earth subsystems with a reduced-form geophysical reprentation of the dynamic subsystem is insightful for decision-makers, both at the global scale for climate policy and at the regional scale for management of the subsystem. Using value function decomposition, we show that the social cost of carbon is increased from SCC to SCCDS by the endogenous subsystem through three main channels: a scaling of the standard channel driving optimal policy by the sign and magnitude of the feedback the subsystem brings to climate change, an insurance channel that measures how subsystem idiosyncratic risk affects aggregate climate risk on intertemporal welfare, and the impact a marginal carbon emissions has on intertemporal welfare through its effect on the future dynamics of the subsystem. Thus, the subsystem has an impact on optimal climate policy that cannot be reduced to the expected value of the feedback it has on climate change. At the regional scale, the explicit reduced-form geophysical representation of subsystem's own dynamics which is nonlinear and partly beyond direct control of the decision-maker allows to study the social cost of the dynamic system SCDS, i.e. the cost of a marginal decrease in subsystem's state because of its reduced ability to self-perpetuate. Our methodological approach could be operationalized for public decision-making regarding other climate subsystems whose fate is debated.

For illustration, we apply our general framework to the fierce debates over the fate of the Amazon rainforest. We use a stochastic climate-economy model with aggregate climate risk over transcient climate response to cumulative emissions and add a stylized reduced-form geophysical dynamics of the rainforest with idiosyncratic stochastic risk over the dynamics of the forest. We move away from the modeling of a generic catastrophe to represent it as an emergent property of the dynamic system. We calibrate the dynamics explicitely and take into account both stochastic risk within climate models and scientific uncertainty over various climate models in our decision criterion. Our approach yields three key results. First, the social cost of carbon should include the impact that a marginal increase in cumulative emissions at the global scale has on the dynamics of the rainforest. This includes both a scaling of current policy by the carbon releases from the Amazon rainforest under changing climate

and an insurance channel because the carbon releases have not the same social value depending on the states of the world where they occur. This also includes the marginal value of a carbon emission on intertemporal welfare through its impact on future subsystem's dynamics. Second, the social value of the Amazon rainforest as a carbon stock cannot be reduced to the amount of carbon it contains: the SCDS matters too, as it represents a significant share of the SCC under expected utility and standard aggregate climate risk. Third, risk and scientific uncertainties are key components of these subsystems: decision-making should account for them in the decision process rather than averaging over deterministic realizations. This means first and foremost taking risk seriously in our modeling approch, with global solution methods and multiple sources of risk interacting. Finally, it means offering the general public decision-making tools that are flexible in terms of attitudes to scientific risk and uncertainty, such as the smooth amiguity criterion. Both SCCDS and SCDS increase sharply with these preference parameters under our robust social choice criterion.

Our results yield three key policy insights at the global scale, from global to regional scales and at the regional scale respectively. First, decision-makers should use SCCDS instead of SCC, i.e. augment the SCC from the impact of a marginal emissions on the Amazon rainforest, that further releases carbon. Emitters around the world should pay around 15% per tCO_2 for the welfare impact of their emissions on the rainforest. Second, the wedge between SCCDS and SCC, i.e. between the SCC without endogenous Amazon rainforest and the SCCDS with this additional feedback, could be leveraged around the world and used to finance payment for ecosystem services for the preservation of the rainforest in a double dividend fashion. These mechanisms are the cornerstone of the UN-sponsored REDD+ strategy. The wedge could address the challenge of financing these coasian subsidies for not deforesting by clearly identifying who is responsible for what in this subsystem's dynamics whose fate is not entirely under the control of the governments of the territory in which they are located. Indeed, when multiplied by the universe of carbon emissions, a 15% increase in the SCC at the global scale represent an amount far larger than any other source of funding proposed so far. Third, the social value given to an hectare of rainforest should include not only the standard social cost of carbon SCC, but the sum of the amazon-augmented social cost of carbon SCCDS and the subsystem channel of the social cost of the dynamic system SCDS. This subsystem channel of the SCDS represents around 9% of the standard SCC obtained under aggregate climate risk. Indeed, a marginal decrease in the forest cover has a first-order welfare impact, as it releases carbon, but also a second-order impact on the future dynamics of the subsystem as a whole. Our theoretical work can

therefore be operationalized in local cost-benefit analysis of deforestation and be used in complement to the significant progress in the quantification of carbon stored at the finest scale via satellite observation. We show that, considering only its value as a carbon stock, the value of a hectare of rainforest is 24% higher than the value currently used in cost-benefit analysis. This SCDS is also interesting to differentiate between different subsystems and understand how these differences bring differences in terms of optimal policy at the global and the regional scales. The dynamics of the Amazon rainforest, which includes a feedback effect, is different from other tropical rainforests (Staal et al., 2020): feedback dynamics are weaker for Congo rainforest and southeast Asian rainforests are not vulnerable to forest-rainfall feedbacks because of their maritime climate zones. Incorporating an explicit geophysical dynamics of the subsystem also matters for risk ranking among various climate subsystems.

Our work has limitations. Some limitations are standard in this literature, for instance the simple representation of the macroeconomy. Two key limitations are related to our specific modeling choices regarding the rainforest: on its dynamics and on its valuation. First, there are more uncertainties at stake with the future of the Amazon rainforest than the one we consider. Here, we have tried to grasp some of this deep uncertainty to show how it influences our results. Second, the main limitation and way forward would be to include other values to the subsystems. For the Amazon rainforest, we focus on the use value of the rainforest as a global carbon stock and abstract from other values: direct use values e.g. timber products, indirect use value e.g. water and nutrient recycling, option and existence value, rights of the indigenous people, intrinsic value. Doing so, we could study how subsystem's idiosyncratic risk interacts with standard macroeconomic risk at the continental scale, for instance when the rainforest has other externalities such as health impacts that may affect economic growth at the continental scale. Integrating all these values is left for future research.

A Appendix

A.1 Analytical decomposition - SCC

Expected utility A second-order Taylor expansion around $z := (\mathbb{E}_t(A_{t+1}), \mathbb{E}_t(T_{t+1}))$ writes:

$$\begin{aligned}
\mathbb{E}_t\left(\frac{\partial U_{t+1}}{\partial T_{t+1}}\right) \approx & \left.\frac{\partial U_{t+1}}{\partial T_{t+1}}\right|_z \text{ (zeroth-order)} \\
& + \left.\frac{\partial^2 U_{t+1}}{\partial^2 T_{t+1}}\right|_z \mathbb{E}_t\left(T_{t+1} - \mathbb{E}_t(T_{t+1})\right) \text{ (first-order)} \\
& + \left.\frac{\partial^2 U_{t+1}}{\partial T_{t+1}\partial A_{t+1}}\right|_z \mathbb{E}_t\left(A_{t+1} - \mathbb{E}_t(A_{t+1})\right) \text{ (first-order)} \\
& + \frac{1}{2}\left.\frac{\partial^3 U_{t+1}}{\partial^2 T_{t+1}\partial A_{t+1}}\right|_z \mathbb{E}_t\left[\left(A_{t+1} - \mathbb{E}_t(A_{t+1})\right)\left(T_{t+1} - \mathbb{E}_t(T_{t+1})\right)\right] \text{ (second-order)} \\
& + \frac{1}{2}\left.\frac{\partial^3 U_{t+1}}{\partial^2 T_{t+1}\partial A_{t+1}}\right|_z \mathbb{E}_t\left[\left(T_{t+1} - \mathbb{E}_t(T_{t+1})\right)\left(A_{t+1} - \mathbb{E}_t(A_{t+1})\right)\right] \text{ (second-order)} \\
& + \frac{1}{2}\left.\frac{\partial^3 U_{t+1}}{\partial T_{t+1}\partial^2 A_{t+1}}\right|_z \mathbb{E}_t\left[\left(A_{t+1} - \mathbb{E}_t(A_{t+1})\right)\left(A_{t+1} - \mathbb{E}_t(A_{t+1})\right)\right] \text{ (second-order)} \\
& + \frac{1}{2}\left.\frac{\partial^2 U_{t+1}}{\partial^3 T_{t+1}}\right|_z \mathbb{E}_t\left[\left(T_{t+1} - \mathbb{E}_t(T_{t+1})\right)\left(T_{t+1} - \mathbb{E}_t(T_{t+1})\right)\right]) \text{ (second-order)}
\end{aligned} \tag{11}$$

The first-order terms are all zero. Indeed, the expectation passes through because the first part of each first-order term is not random as well as the zeroth-order term. The last second-order term is zero for the same reason. The second part of the first and the second second-order term correspond to $cov(T_{t+1}, A_{t+1})$. The second part of the third second-order term is $var(A_{t+1})$. That yields:

$$\mathbb{E}_t\left(\frac{\partial U_{t+1}}{\partial T_{t+1}}\frac{\partial T_{t+1}}{\partial S_{t+1}}\right) = \mathbb{E}_t\left(\frac{\partial U_{t+1}}{\partial T_{t+1}}\right)\mathbb{E}_t\left(\frac{\partial T_{t+1}}{\partial S_{t+1}}\right) + cov\left(\frac{\partial U_{t+1}}{\partial T_{t+1}}; \frac{\partial T_{t+1}}{\partial S_{t+1}}\right) \tag{12}$$

$$\mathbb{E}_t\left(\frac{\partial U_{t+1}}{\partial T_{t+1}}\right) \approx \left[\underbrace{\left.\frac{\partial U_{t+1}}{\partial T_{t+1}}\right|_z}_{CE} + \underbrace{\left.\frac{\partial^3 U_{t+1}}{\partial^2 T_{t+1}\partial A_{t+1}}\right|_z cov(T_{t+1}, A_{t+1}) + \frac{1}{2}\left.\frac{\partial^3 U_{t+1}}{\partial T_{t+1}\partial^2 A_{t+1}}\right|_z var(A_{t+1})}_{PC}\right] \tag{13}$$

We want to decompose all future components of SCCDS. Starting from equation (1) that defines optimal policy under expected utility. We assume that we are at the optimum and simplify notations for the expectations. There is no decay, so that we have:

$$V^a_{1,t} = \mathbb{E}_t\left(\frac{\partial U_{t+1}}{\partial T_{t+1}}\frac{\partial T_{t+1}}{\partial S_{t+1}}\right) = \mathbb{E}_t\left(u'_S[c_{t+1}]\right) + \delta V^a_{1,t+1}V^b_{1,t+1} + \delta V^c_{1,t+1} + \delta V_{2,t+1} \tag{14}$$

$$V^a_{1,t} = \mathbb{E}_t\left(u'_S[c_{t+1}]\right) + \delta V^c_{1,t+1} + \delta V_{2,t+1} + \delta V^a_{1,t+1}V^b_{1,t+1} \tag{15}$$

Eventually advancing this equation and inserting it in itself yields:

$$V^a_{1,t} = \mathbb{E}_t\left(u'_S[c_{t+1}]\right) + \delta V^c_{1,t+1} + \delta V_{2,t+1} + \delta V^b_{1,t+1}\left(\mathbb{E}_t\left(u'_S[c_{t+2}]\right) + \delta V^c_{1,t+2} + \delta V_{2,t+2} + \delta V^a_{1,t+2}V^b_{1,t+2}\right) \tag{16}$$

Assuming that the shadow value of carbon concentration increase $\partial U/\partial S$ converges to 0 over our large time horizon and along an optimal path, we repeatedly avance and insert this equation in itself. Then, inserting this in equation (4), and repeating the operation, yields equation (6) that includes all future components.

Smooth ambiguity One can extend the conclusion made here under expected utility to our smooth ambiguity criterion. The SCC^{SA} and SCCDS^{SA} write:

$$SCC_t^{SA} = \frac{\delta}{u_c'(c_t)} \frac{\partial V_{t+1}}{\partial T_{t+1}} \frac{\partial T_{t+1}}{\partial S_{t+1}} \tag{17}$$

$$SCCDS_t^{SA} = \frac{\delta}{u_c'(c_t)} a_t \mathbb{E}_{\chi_t} \left(b_t \mathbb{E}_{\pi_t} \left[d_t \left(\overbrace{\left[\frac{\partial V_{t+1}}{\partial T_{t+1}} \frac{\partial T_{t+1}}{\partial S_{t+1}} \left(1 + \frac{\partial S_{t+1}}{\partial A_{t+1}} \frac{\partial A_{t+1}}{\partial S_t} \right) \right] + \left[\frac{\partial V_{t+1}}{\partial A_{t+1}} \frac{\partial A_{t+1}}{\partial T_t} \frac{\partial T_t}{\partial S_t} \right]}^{Channels\ from\ main\ text} \right) \right] \right) \tag{18}$$

$$\text{where } a_t(x) = (u \circ h^{-1})' \mathbb{E}_{\chi_t} \left((h \circ v^{-1}) \mathbb{E}_{\pi_t} (v \circ u^{-1})(x) \right.$$

$$b_t(x) = \left((h \circ v^{-1})' \mathbb{E}_{\pi_t} (v \circ u^{-1})(x) \right.$$

$$d_t(x) = (v \circ u^{-1})'(x)$$

We use standard operations on expectations:

$$\begin{aligned} SCCDS_t^{SA} = & \frac{\delta}{u_c'(c_t)} \overbrace{a_t \left[\mathbb{E}_{\chi_t} (b_t \mathbb{E}_{\pi_t} (d_t)) \right]}^{Scaling} \mathbb{E}_{\chi_t, \pi_t} \left(\frac{\partial V_{t+1}}{\partial T_{t+1}} \frac{\partial T_{t+1}}{\partial S_{t+1}} \left(1 + \frac{\partial S_{t+1}}{\partial A_{t+1}} \frac{\partial A_{t+1}}{\partial S_t} \right) + \left[\frac{\partial V_{t+1}}{\partial A_{t+1}} \frac{\partial A_{t+1}}{\partial T_t} \frac{\partial T_t}{\partial S_t} \right] \right) \\ & + \frac{\delta}{u_c'(c_t)} \underbrace{a_t cov \left[b_t \mathbb{E}_{\pi_t} (d_t); \mathbb{E}_{\pi_t} \left(\frac{\partial V_{t+1}}{\partial T_{t+1}} \frac{\partial T_{t+1}}{\partial S_{t+1}} \left(1 + \frac{\partial S_{t+1}}{\partial A_{t+1}} \frac{\partial A_{t+1}}{\partial S_t} \right) + \left[\frac{\partial V_{t+1}}{\partial A_{t+1}} \frac{\partial A_{t+1}}{\partial T_t} \frac{\partial T_t}{\partial S_t} \right] \right) \right]}_{Temporal\ resolution\ of\ uncertainty\ (TRU_t)} \\ & + \frac{\delta}{u_c'(c_t)} \underbrace{a_t \mathbb{E}_{\chi_t} \left[b_t cov \left(d_t; \frac{\partial V_{t+1}}{\partial T_{t+1}} \frac{\partial T_{t+1}}{\partial S_{t+1}} \left(1 + \frac{\partial S_{t+1}}{\partial A_{t+1}} \frac{\partial A_{t+1}}{\partial S_t} \right) + \left[\frac{\partial V_{t+1}}{\partial A_{t+1}} \frac{\partial A_{t+1}}{\partial T_t} \frac{\partial T_t}{\partial S_t} \right] \right) \right]}_{Temporal\ resolution\ of\ risk\ (TRR_t)} \end{aligned} \tag{19}$$

In other words, the channel derived under expected utility is scaled with:

$$a_t \mathbb{E}_{\chi_t} (b_t \mathbb{E}_{\pi_t} (d_t))) = \underbrace{\left(\mathbb{E}_{\chi_t} \left[\mathbb{E}_{\pi_t} ((1-\theta) V_{t+1})^{\frac{1-\gamma}{1-\theta}} \right]^{\frac{1-\mu}{1-\gamma}} \right)^{\frac{\mu-\theta}{1-\mu}}}_{a_t} \mathbb{E}_{\chi_t} \left[\underbrace{\left(\mathbb{E}_{\pi_t} [(1-\theta) V_{t+1}]^{\frac{1-\gamma}{1-\theta}} \right)^{\frac{\gamma-\mu}{1-\gamma}}}_{b_t} \mathbb{E}_{\pi_t} \underbrace{([1-\theta] V_{t+1})^{\frac{\theta-\gamma}{1-\theta}}}_{d_t} \right] \tag{20}$$

The scaling does not affect the relative magnitude of the channels derived in equation (6) but the concave transformation increases the SCCDS. Thus, the conclusion made under expected utility on the relative magnitude of insurance in optimal policy applies under the smooth ambiguity criterion. Note that the scaling equals one when $\mu = \eta = \gamma$, which yields expected utility. It is well known that

the dynamic models of ambiguity aversion yield timing nonindifference (Strzalecki, 2013), i.e. preference for the timing of resolution of risk and preference for the timing of resolution of uncertainty. The second line of equation (19) is the preference for temporal resolution of uncertainty and writes:

$$TRU_t = \left(\mathbb{E}_{\chi_t}\left[\mathbb{E}_{\pi_t}((1-\theta)V_{t+1})^{\frac{1-\gamma}{1-\theta}}\right]^{\frac{1-\mu}{1-\gamma}}\right)^{\frac{\mu-\theta}{1-\mu}} cov\left(\left(\mathbb{E}_{\pi_t}[(1-\theta)V_{t+1}]^{\frac{1-\gamma}{1-\theta}}\right)^{\frac{\gamma-\mu}{1-\gamma}}\mathbb{E}_{\pi_t}\left([1-\theta]V_{t+1}\right)^{\frac{\theta-\gamma}{1-\theta}}; \frac{\partial V_{t+1}}{\partial T_{t+1}}\frac{\partial T_{t+1}}{\partial S_{t+1}}\left(1+\frac{\partial S_{t+1}}{\partial A_{t+1}}\frac{\partial A_{t+1}}{\partial S_t}\right)+\left[\frac{\partial V_{t+1}}{\partial A_{t+1}}\frac{\partial A_{t+1}}{\partial T_t}\frac{\partial T_t}{\partial S_t}\right]\right) \quad (21)$$

This channel increases (decreases) the SCC^{SA} and SCCDS^{SA} when $\mu \geq (\leq)\theta$, i.e. when the planner has preference for early (late) resolution of uncertainty, which is the case for all values of μ and θ explored. The third line of equation (19), already depicted in Lemoine and Rudik (2017) under Epstein-Zin-Weil preferences, is preference for temporal resolution of risk (see also Lemoine (2021)) and writes:

$$TRR_t = \left(\mathbb{E}_{\chi_t}\left[\mathbb{E}_{\pi_t}((1-\theta)V_{t+1})^{\frac{1-\gamma}{1-\theta}}\right]^{\frac{1-\mu}{1-\gamma}}\right)^{\frac{\mu-\theta}{1-\mu}} \mathbb{E}_{\chi_t}\left[\left(\mathbb{E}_{\pi_t}[(1-\theta)V_{t+1}]^{\frac{1-\gamma}{1-\theta}}\right)^{\frac{\gamma-\mu}{1-\gamma}} cov\left(\left([1-\theta]V_{t+1}\right)^{\frac{\theta-\gamma}{1-\theta}}; \frac{\partial V_{t+1}}{\partial T_{t+1}}\frac{\partial T_{t+1}}{\partial S_{t+1}}\left(1+\frac{\partial S_{t+1}}{\partial A_{t+1}}\frac{\partial A_{t+1}}{\partial S_t}\right)+\left[\frac{\partial V_{t+1}}{\partial A_{t+1}}\frac{\partial A_{t+1}}{\partial T_t}\frac{\partial T_t}{\partial S_t}\right]\right)\right] \quad (22)$$

This channel increases (decreases) the SCC^{SA} and SCCDS^{SA} when $\gamma \geq (\leq)\theta$, i.e. when the planner has preference for early (late) resolution of risk, which is the case for all values of γ and θ explored here.

A.2 Analytical decomposition - Social cost of the dynamic subsystem

Smooth ambiguity Under this social choice criterion, the SCDS^{SA} writes:

$$SCDS_t^{SA} = \frac{\delta}{u_c'(c_t)}a_t\mathbb{E}_{\chi_t}\left(b_t\mathbb{E}_{\pi_t}\left[d_t\left(\overbrace{\left(\frac{\partial V_{t+1}}{\partial T_{t+1}}\frac{\partial T_{t+1}}{\partial S_{t+1}}\frac{\partial S_{t+1}}{\partial A_{t+1}}\right)+\mathbb{E}_t\left(\frac{\partial V_{t+1}}{\partial A_{t+1}}\right)}^{Channels\ from\ main\ text}\right)\right]\right) \quad (23)$$

The same interpretation as equation (19) above applies to the SCDS^{SA}.

A.3 Resolution of the model

Simplicial Chebyshev Approximation. We use a simplicial complete Chebyshev approximation in the three-dimensional state space. Denote a d-dimensional hyperrectangle state space $[\mathbf{x}_{min}, \mathbf{x}_{max}]$ as $\{\mathbf{x} = (x_1, ..., x_d) : x_{min,j} \leq x_j \leq x_{max,j}, j = 1, ..., d\}$ with d = 3 and where $\mathbf{x}_{min,j}$ and $\mathbf{x}_{max,j}$ are lower and upper bounds of state variable x_j. The state variables are A, T and K (from which Y can be deduced). The time-dependent approximation space is defined around a deterministic growth path derived from Ramsey formula. This adaptive grid allows to use fewer collocation points than on a standard hyperrectangle grid. We do not use a complete Chebyshev approximation as it assumes

symmetric approximation in each dimension. In our multidimensional problem, the value functions have higher curvature in the forest and temperature dimensions because of the feedback effect, while savings rate is fixed and capital dynamics smooth: we use degree-3, degree-4, degree-6 interpolation for capital, temperature and Amazon respectively. We do not have a proper kink so we do not use adaptive sparse grids (Brumm and Scheidegger, 2017) and stick to a tensor product grid that can handle our curvature. The approximation writes:

$$\hat{V}(\mathbf{x}, \mathbf{b}) = \sum_{\alpha \geq 0, \sum_{j=1}^{d} \alpha_j / n_j \leq 1} b_\alpha \Phi_\alpha(\mathbf{x}) \tag{24}$$

where n_j is the maximal degree in dimension j and Φ the product of one-dimensional Chebyshev basis functions $\tau_{\alpha_i}(Z_i(x_i)) = cos(\alpha_i cos^{-1}(Z_i(x_i))$ where we have that $Z_j(x_j) = \frac{2x_j - x_{max,j} - x_{min,j}}{x_{max,j} - x_{min,j}}$ for $j = 1, ..., d$. Φ writes:

$$\Phi_\alpha(\mathbf{x}) = \prod_{i=1}^{d} \tau_{\alpha_i}(Z_i(x_i)) \tag{25}$$

Chebyshev nodes To get a not-overfitted approximation, the number of nodes, m, should not be less than the number of unknown coefficients, b_α. Choosing tensor-grids may lead to another level of curse of dimensionality. We chose Chebyshev nodes and let $m_j = n_j + 1$, so that the number of grids in dimension j is equal to one plus the maximal degree of Chebyshev approximation in dimension j. For our d-dimensional problem in the state space $[\mathbf{x}_{min}, \mathbf{x}_{max}]$, there are $m_1 * m_2 * ... * m_d$ approximation nodes with the tensor grid and the values of Chebyshev nodes in dimension j are :

$$x_{i,j} = (z_{i,j} + 1)(x_{max,j} - x_{min,j})/2 + x_{min,j} \tag{26}$$

with $z_{i,j} = -cos((2i-1)\pi/(2m_j))$ for $i = 1, ..., m_j$. Furthermore, we break the 'curse-of-dimensionality' on tensor grids using CPU parallel computing as the interpolation can be done independently between the different approximation nodes.

Terminal value The calculation is done on a finite horizon (T = 500 years) as an approximation of the infinite program. The terminal value is defined as the sum of all the period utilities from time T to infinity. The assumption made is that the consumption will grow for a constant capital per efficient capita and total abatement, with a deterministic path for the capital derived from Ramsey. The terminal constraint uses a modified discount factor (Barr and Manne, 1967). The choice of the terminal value does not affect the program : a 10% increase in the terminal value does not significantly affect the optimal path. It writes:

$$TVF = \left(\frac{1 - t_s tep}{1 - \delta(1+g)^\theta} \right)^{\frac{1}{\theta}} u(\bar{c}) \tag{27}$$

with $\bar{c}$ the consumption for constant capital per efficient capita and total abatement, δ the discount rate, g the growth rate of labour productivity from the last period,

We use deforestation rates from Aguiar et al. (2016): (km^2 / year) decreasing to 3900 (2020) then to 1000 (2025) and stabilizing until 2050 (scenario A), decreasing to 3900 (2020) and stabilizing until 2050 (scenario B), increasing to 15000 (2020) and stabilizing until 2050 (scenario C). The calibration of our dynamics is a two-step procedure. First, we calibrate externally the maximum impact of local temperature changes on tree carbon losses through droughts $\bar{\epsilon}$. We use projections from climate models at a fine spatial resolution to derive a relationship between changes in local temperatures and changes in a drought index over the Amazon basin, the maximum cumulative water deficit (MCWD) anomaly with respect to an historical baseline. We use past observations to derive a link between MCWD and carbon losses. Then, we calibrate the whole distribution of $\tilde{\epsilon}$ within the support [0 ; $\bar{\epsilon}$] internally so that the dynamics of our system matches the expert assessments from Kriegler et al. (2009) on a possible tipping point. A taste of the uncertainty between models appear on the graph below:

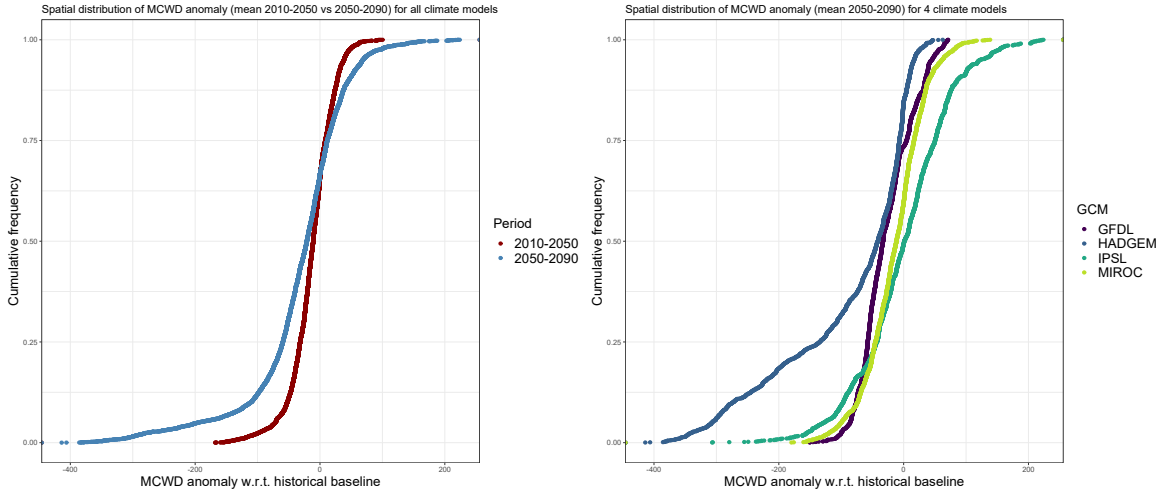

Figure 5: Spatial cumulative distribution at 0.5° resolution of maximum cumulative water deficit anomaly with respect to historical baseline for RCP 8.5 over the Amazon rainforest. **Left** shows that over all climate models, the average MCWD anomaly shifts to more extreme and frequent droughts from 2010-2050 to 2050-2090. **Right** shows how the distribution of average MCWD anomaly over 2050-2090 depends on the climate model used

A.5 Calibration

A.5.1 External calibration

Step 1 - Prepare and match datasets We use an Amazon shapefile (Silva-Souza and Souza, 2020) at a 0.5° x 0.5° spatial resolution and calculate for each cell the MCWD anomaly observed along three representative concentration pathways (RCPs 2.6, 6.0, 8.5) in comparison with the historical baseline (1984-2004 as in Phillips et al. (2009)). We use projections from climate models taken from the Inter-Sectoral Impact Model Intercomparison (ISIMIP) for local precipitations and temperatures. For each RCP, we use fixed year-2005 land use, nitrogen deposition and fertilizer input to avoid double counting of human direct influences on the forest, as we already take into account deforestation and degradation. We use the estimates taken from one type of model: the hydrological model MATSIRO. We use all climate impact models available as the main climate uncertainty on future droughts stems from the differences between these models: GFDL-ESM2M, HadGEM2-ES, IPSL-CM5A-LR, MIROC5. Two other types of models could be used: dynamic global vegetation models and land surface models. But we do not have RCP trajectories for the dynamic global vegetation model and we do not have historical baseline for CLM45: we would have to use fixed-2005 socioeconomic scenarios for the historical baseline. Furthermore, land-surface models are not appropriate for the study of the impact of droughts on the rainforest and the vegetation models assume fixed tree mortality while we want to use historical data (Phillips et al., 2009) to describe the link between droughts and carbon losses.

We transform precipitation data from kg/m^{-2}/s^{-1} to mm^2/month. With P the precipitation level in mm^2/month, the cumulative water deficit (CWD) writes[6] (Papastefanou et al., 2020),with m the months, k the grid cells (m = 1,..., 12) and i the climate model used:

$$CWD_{k,m,i} = CWD_{k,m-1,i,RCP} + P_{k,m,i} - 100 \text{ if } P_{k,m,i,RCP} < 100 \tag{30}$$

$$CWD_{k,m,i} = 0 \text{ if } P_{k,m,i} > 100 \text{ and } CWD_{k,0,i} = 0 \tag{31}$$

We calculate MCWD for each year (y) from october n to september n+1 for each cell k. We have: $MCWD_{k,y,RCP,i} = min(CWD_{k,m,RCP,i})$, $m = 1,...,12$. We obtain the MCWD anomaly, in com-

[6] A fixed value for evapotranspiration (ET) of 100 mm per month is used. When monthly rainfall is below 100 mm, the forest is under water deficit.

parison with the mean values taken from the baseline calculated at the cell level: $MCWD^{anomaly}_{k,y,RCP,i} = MCWD_{k,y,RCP,i} - MCWD^{baseline}_{k,RCP,i}$. We use local surface temperature data from all climate impact models along the three RCP and match it to the data on MCWD anomaly at the pixel level. We calculate the mean average local surface temperature from october n to september n+1. We translate the MCWD anomaly to carbon losses. We take observations from previous literature (Phillips et al., 2009) to derive a simple link c (c $\approx$ 0.05 tC/ha/y/mm^2 MCWD anomaly) between yearly MCWD anomaly (in mm^2) and the carbon losses observed (in tC / ha / year). The carbon losses observed depend on the size of the pixel, but the difference in size is minor ($< 3\%$) and we focus on the difference in carbon stored. We take data from EarthData (NASA) for the carbon storage spatial heterogeneity (Baccini et al., 2012). We scale each C_i by the ratio of the carbon stock of this pixel i to the mean of the carbon stock in every pixel to take into account heterogeneity in the distribution of carbon stored.

Step 2 - Econometrics model selection and tests We have a balanced panel dataset with yearly projections of carbon losses and local temperatures from october 2006 to september 2099 (T=93) for each location (N depends on the climate impact model used but overall, N $>>$ T). The basic OLS regression model does not consider heterogeneity across locations or across years. We use fixed effects models as the Durbin-Wu-Hausman test is rejected for each model: while the fixed effect specification has a cost in terms of degrees of freedom, using random effects modelling would come with the too heavy assumption that the unobserved heterogeneity of the model is not correlated with the regressors. We check if time fixed effects are needed with Lagrange multiplier tests and F test: we reject the null hypothesis and add T-1 (to avoid perfect multicollinearity) time fixed effects to our fixed effects panel specification. Our specification limits the probability of coefficients being driven by omitted variables. We do not differentiate the data as stationarity is not a problem in our panel dataset with time fixed effects and N $>>$ T. We are not preoccupated by simultaneity as local temperatures are mainly driven by global cumulative emissions stock as long as the vegetation cover is not fully depleted. We test homoskedasticity and serial correlation with Breusch-Pagan and Breusch-Godfrey lagrange multipliers tests. We reject the null hypothesis and find evidence of heteroskedasticity and serial correlation: we might use robust covariance matrix estimators à la White for our standard errors but first need to test for cross-sectional dependence with Pesaran's and Breusch-Pagan's tests. As expected (spatial data), we reject the null hypothesis that residuals are not correlated so that there is cross-sectional dependence in each model, which might bias our coefficients. Furthermore, we use Driscoll and Kraay (1998) standard errors to account for this dependence structure. We also add

regional fixed effects to account for heterogeneity in the vegetation. We use Silva-Souza and Souza (2020) woody plant regionalization into 13 subregions based on k-means partitioning. Let C be the carbon losses (in tC / ha / y), X the local temperature at the pixel level, u the error term, i the notation for our geo-coded entity, t the notation for time, r the Silva-Souza and Souza (2020) subregions. β is our coefficient of interest, α, δ and ζ vectors of location, time and region fixed effects respectively. We estimate the following:

$$C^j_{i,r,t} = \beta^j X^j_{i,r,t} + \alpha^j_i + \delta^j_t + \zeta^j_r + u^j_{i,r,t} \tag{32}$$

We have our coefficients of interest $\hat{\beta}^j$ for each model j that gives how a 1°C increase in local temperature translates into a change in carbon stored (in tC / ha / year).

Specification	Climate model	Coefficient	Standard Errors [robust]	t-value [robust]
FE	HADGEM	-1.1271	0.0031 [0.0226]	-365.806 [-49.8816]
	GFDL	-2.7006	0.0056 [0.025]	-484.8025 [-108.1676]
	IPSL	-0.4885	0.0043 [0.0133]	-114.0374 [-36.7257]
	MIROC	-1.1996	0.0036 [0.0225]	-332.0498 [-53.2061]
FE & year FE	HADGEM	-1.4039	0.0048 [0.0288]	-293.4842 [-48.7659]
	GFDL	-3.0708	0.0067 [0.0262]	-454.942 [-117.3824]
	IPSL	-0.7977	0.007 [0.0204]	-113.5831 [-39.1795]
	MIROC	-1.6436	0.0049 [0.0311]	-335.25 [-52.9338]
FE & regional FE	HADGEM	-1.1271	0.0031 [0.0563]	-365.806 [-20.0358]
	GFDL	-2.7006	0.0056 [0.1559]	-484.8025 [-17.3256]
	IPSL	-0.4885	0.0043 [0.1107]	-114.0374 [-4.4126]
	MIROC	-1.1996	0.0036 [0.0892]	-332.0498 [-13.45]
FE, year & regional FE	HADGEM	-1.4039	0.0048 [0.0048]	-293.4842 [-293.4842]
	GFDL	-3.0708	0.0067 [0.0067]	-454.942 [-454.942]
	IPSL	-0.7977	0.007 [0.007]	-113.5831 [-113.5831]
	MIROC	-1.6436	0.0049 [0.0049]	-335.25 [-335.25]

We multiply this coefficient by the size ($\approx$ 705 million ha) of the forest (Souza-Rodrigues, 2019) and by the number of years per period (5 years) and express it as a share of the carbon stored in the forest at initial time that can be lost (75GtC (Armstrong McKay et al., 2022)). This coefficient gives the upper bound of the mean additional share of carbon stored in the rainforest that is released per period because of droughts for a one degree increase in local temperature in climate model j. Our coefficients ϵ_j are taken from observations of the 2005 drought (Phillips et al., 2009), one of the most severe droughts observed over the Amazon so far. Thus, we assume that $\bar{\epsilon}_j$ are higher estimates of the possible impact of droughts. We assume that on a given period, the impact of droughts on the carbon storage follows a beta distribution of unknown parameters α_s and β_s with support $[0 : \bar{\epsilon}_j]$.

A.5.2 Internal calibration

Data processing We use expert assessments from Kriegler et al. (2009) to calibrate our global dynamics: we calibrate the growth rate g_0, the feedback effect Υ and the parameters α_s and β_s of the beta distribution of stochastic droughts $\tilde{\epsilon}$ to recover the same probabilities of tipping along three RCP. We want to make sure that our dynamic system is approximately in line with these expert elicitations. In the low temperature corridor, the central weighted estimate from core experts in Kriegler et al. (2009) is a probability of 24% of tipping. In the medium temperature corridor, their central estimate is a probability of 49% of tipping. In the high temperature corridor, the central estimate is a probability of 67%. The temperature corridors used by Kriegler et al. (2009) are wide, and we assume fair approximations for their 'low', 'medium' and 'high' temperature corridors are the Shared Socioeconomic Pathways SSP4-3.4, SSP4-6.0, SSP5-8.5. These SSP are available in IPCC AR6 (Smith et al., 2021): more specifically, we use extended SSP as we need data until 2200. The data is available as effective radiative forcing (in W.m^{-2}) time series. We use a simple two-layers box model described in IPCC AR6 (Smith et al., 2021) to translate this data to global average surface temperature:

$$C\frac{d}{dt}\Delta T = \Delta F(t) + \alpha\Delta T - \epsilon\gamma(\Delta T - \Delta T_d) \tag{33}$$

$$C_d\frac{d}{dt}\Delta T_d = \gamma(\Delta T - \Delta T_d) \tag{34}$$

where ΔT (°C) is the temperature change of the surface components of the climate system, ΔT_d (°C) is the temperature change in the deep ocean layer, C and C_d are the effective heat capacities for the surface and deep layers, ϵ is the efficacy of the deep ocean heat uptake and γ is the heat transfer coefficient between the surface and deep layer. We use the central estimates from IPCC for the key parameters and abstract from uncertainty on these parameters[7]. We use Leduc et al. (2016) regional transient climate response to cumulative emissions (2.0°C per TtC over the Amazon basin) and the IPCC (Masson-Delmotte et al., 2021) best estimate for global transient climate response to cumulative emissions (1.65°C per TtC) to have a simple mapping from global to regional temperature.

Jointly calibrate the parameters and distribution of ϵ Reasonable ranges for Υ, the temperature difference between bare soil and forest, range from 3.98 (forest-to-pasture) to 7.06 (forest-to-cropland) in Silvério et al. (2015). Ritchie et al. (2021) use 5. The distribution is chosen so that the

[7] C = 8.1 $\pm$ 1 W.yr.m^{-2} °C^{-1}, C_d = 110$\pm$ 63 W.m^{-2} °C^{-1}, γ = 0.62 $\pm$ 0.13 W.m^{-2} °C^{-1}, ϵ = 1.34 $\pm$ 0.41, α = -1.33 $\pm$ 0.5. We calculate the cumulated sum starting from 1750.

expected value of the mean yearly drought impact over a period is between one half and one fifth of the value of the impact calibrated from the 2005 extreme drought in Phillips et al. (2009). Furthermore, we assume α_s and β_s below 1 to model situations where observations are either close to the upper bound or the lower bound and intermediate values are less likely. This seems reasonable as these extreme droughts seem to occur every five years as observed in the past twenty years, either associated with positive sea surface temperature anomalies in the tropical Atlantic (2005, 2010) or with strong El Niño events (1997/98, 2015/16). Ritchie et al. (2021) use a perturbation rate of 0.2 and a growth rate of 2 so we keep the ratio constant with our perturbation rate ϵ to seek values for which the dynamics fits with experts views. Using the inverse of the cumulative distribution function of our beta distribution of unknown shape α_s and β_s, we give the values of ϵ_{low},ϵ_{medium} and ϵ_{high} that corresponds to the expert probabilities. Then, along the three SSP4-3.4, 4-6.0, 5-8.5, we calibrate g_0, Y, α_s, and β_s, so that in 2200, the dynamic system experiences a dieback for $\epsilon_{low} + \delta$ (same for ϵ_{medium} and ϵ_{high}) but no dieback for $\epsilon_{low} - \delta$ (same for ϵ_{medium} and ϵ_{high}), with $\delta \pm 1\%$. There is a large, potentially infinite number of solutions. Arbitrarily, coefficients are taken to one decimal only and find the ensemble of combinations for which the criteria for convergence are respected. We pick one of the combinations. Our central estimate is: $g_0 = 0.49$, $\alpha_s = 0.36$, $\beta_s = 0.32$, $\mathrm{Y} = 6$. The distribution for ϵ is given in Figure 6:

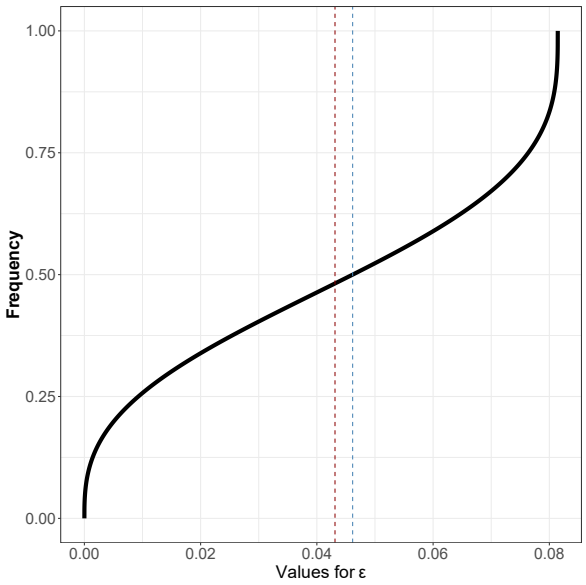

Figure 6: Cumulative distribution function of $\tilde{\epsilon}$ with red mean $\mathbb{E}(\epsilon) \approx 0.0431$ and blue median $\mathbb{P}(\epsilon > 0.0462) = 50\%$.

A.6 Consistency of the coefficients

We run a simulation (1000 paths) of our dynamics for the carbon stored in the rainforest, including all the perturbations, along various extended concentration pathways in Figure (7). We give the mean total carbon net losses (in GtC) for different temperature increases (in °C), with (left) and without (middle) the tipping risk. Finally, we give the same path but under the assumption made in our model that, as there is scientific uncertainty, there is a 50% chance of tipping risk (right). After 2200, we assume that the carbon stored in the forest remains constant: the carbon losses are permanent. In our model, there is no SSP (even the most extreme one) for which there is a dieback of the rainforest before 2100 under deforestation and degradation scenarii.

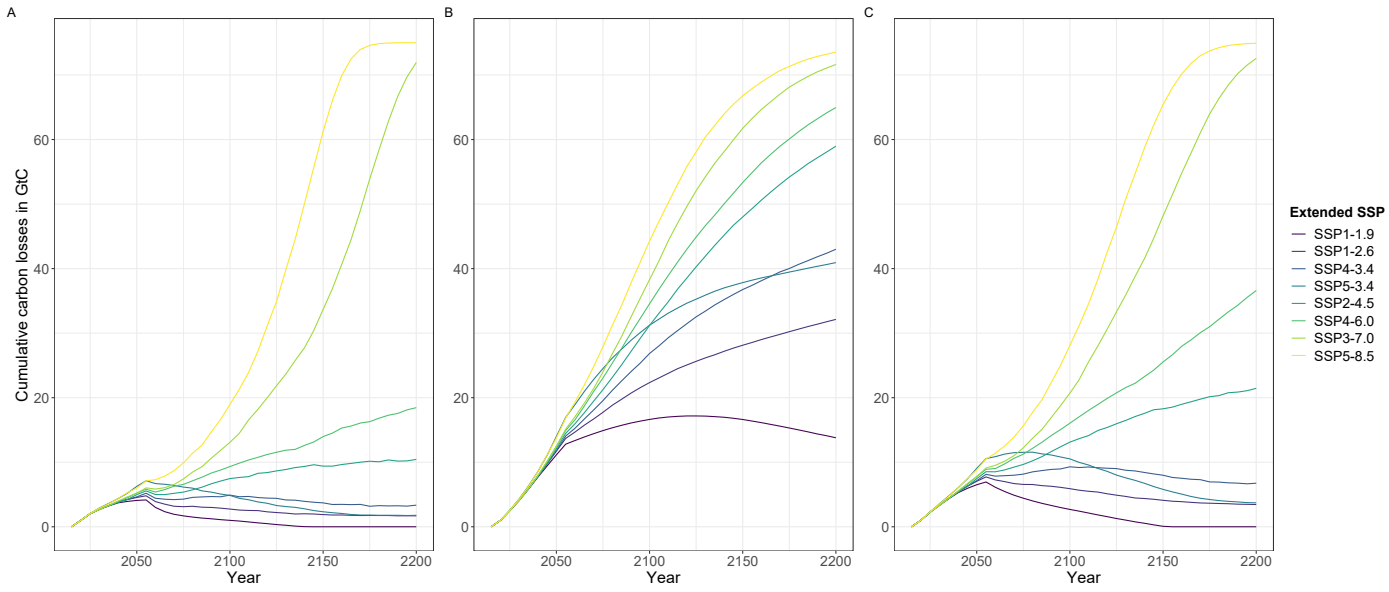

Figure 7: **Time horizon** Mean cumulative carbon losses (in GtC) from the Amazon rainforest along various extended concentration pathways (in °C) from 2000 to 2200 under no tipping risk (A), a tipping risk (B), and in our model (C).

We give the phase diagrams of our dynamic system under no tipping risk and under a tipping risk. The diagrams give for various values of the stochastic impact of temperatures on the dynamics of the rainforest ϵ, over time, and for different scenarii, the change in forest cover with respect to initial period. A dieback of the forest occurs by 2200 only for carbon-intensive scenario that are usually not optimal (so, these scenarii will not occur in our optimized framework), for a tipping risk, and for large values of the impact of global temperatures on the dynamics of the rainforest.

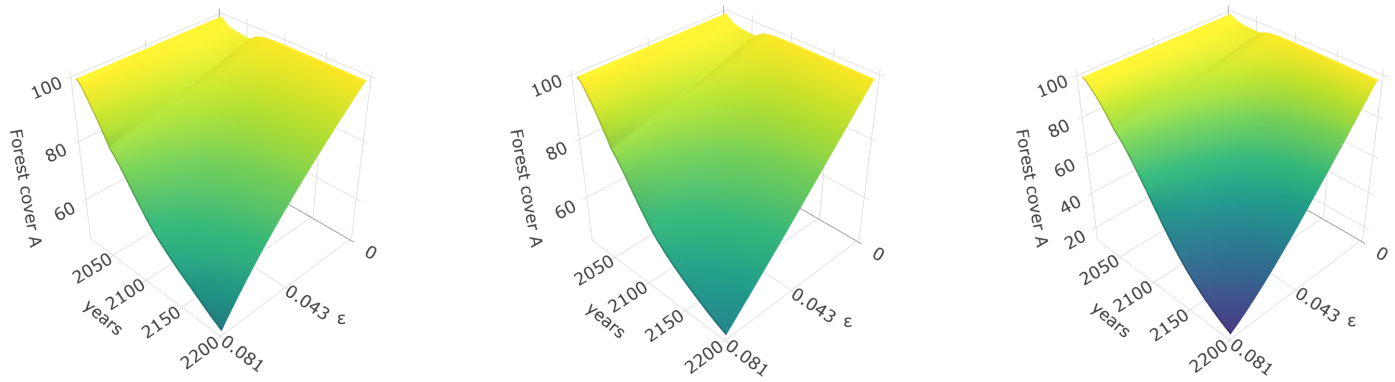

Figure 8: Phase diagram. Dynamics of the forest under no tipping risk for various $\tilde{\epsilon}$ and for a low, medium and a high temperature corridor. $\mathbb{E}(\epsilon) \approx 0.0431$ and $\mathbb{P}(\epsilon > 0.0462) = 50\%$.

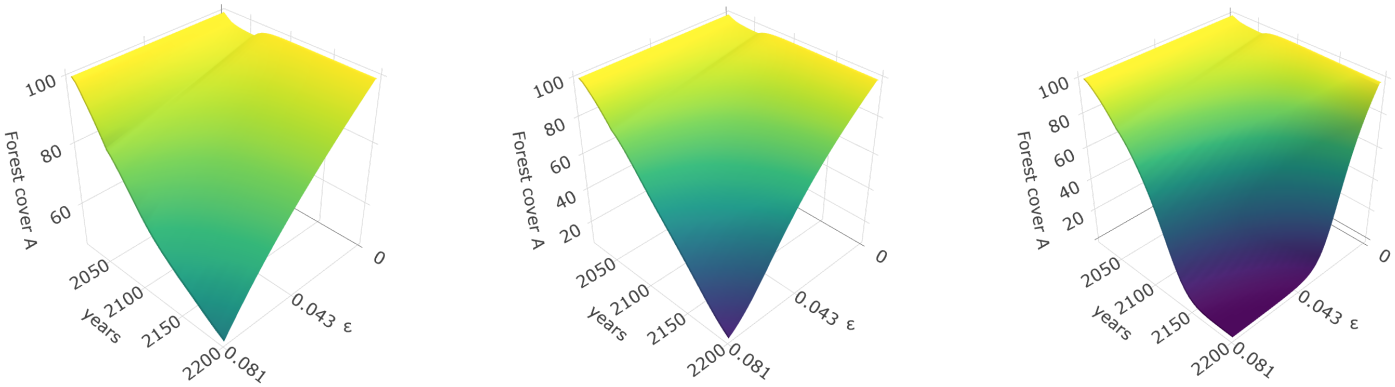

Figure 9: Phase diagram. Dynamics of the forest under a tipping risk, i.e. $\Upsilon \neq 0$, for various $\tilde{\epsilon}$ and for a low, medium and a high temperature corridor. $\mathbb{E}(\epsilon) \approx 0.0431$ and $\mathbb{P}(\epsilon > 0.0462) = 50\%$.

A.7 Stochastic paths for some variables of interest

For three specifications of interest under expected utility, we plot the distribution of stochastic paths until 2100 for temperature increases and forest stock. We also plot the distribution of stochastic paths for abatement rate. These stochastic paths are taken from our optimized intertemporal programs used for the computation of SCC, SCCDS and SCDS under expected utility. In all these graphs, the bold line gives the mean of 100 stochastic paths and the gray area are for 5% and 95% paths.

- Specification 1: benchmark, with aggregate climate risk over transient response to cumulative emissions, but no explicit representation of the amazon rainforest.
- Specification 2: first counterfactual, where there is aggregate climate risk and an explicit representation of the amazon rainforest.

- Specification 3: second counterfactual, where there is both aggregate climate risk and idiosyncratic risk over the dynamics of the rainforest.

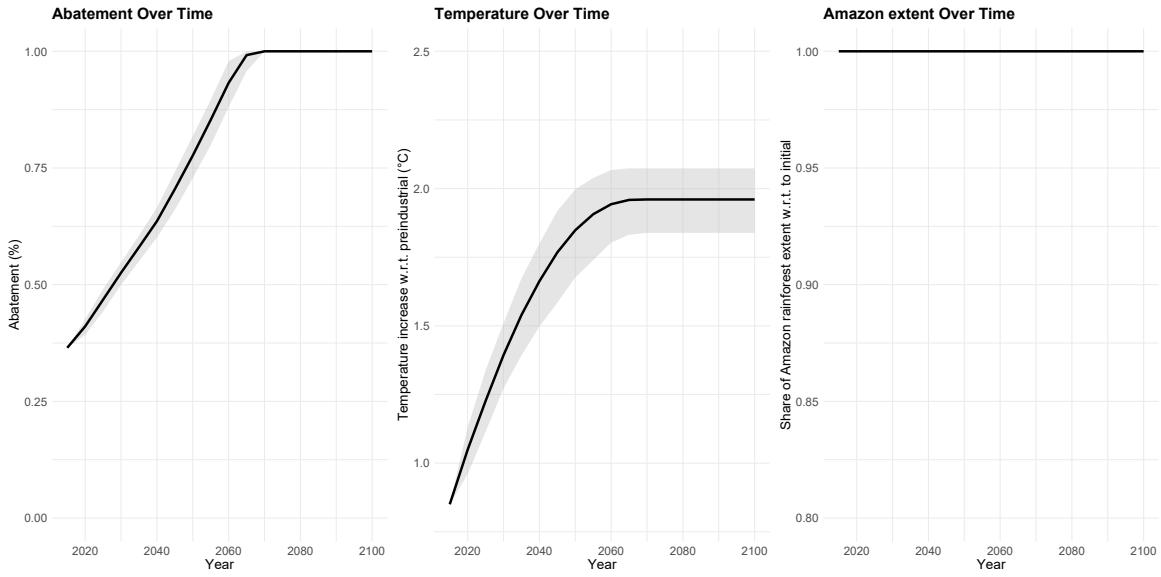

Figure 10: Stochastic optimized paths under aggregate climate risk, without endogenous amazon dynamics.

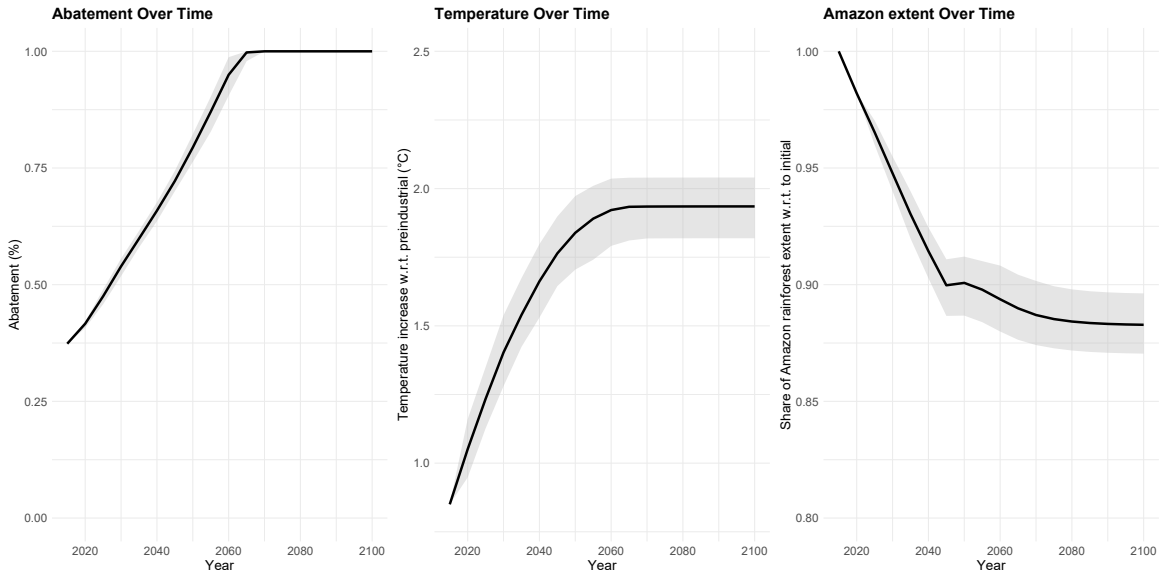

Figure 11: Stochastic optimized paths under aggregate climate risk, with endogenous amazon dynamics, without amazon idiosyncratic risk.

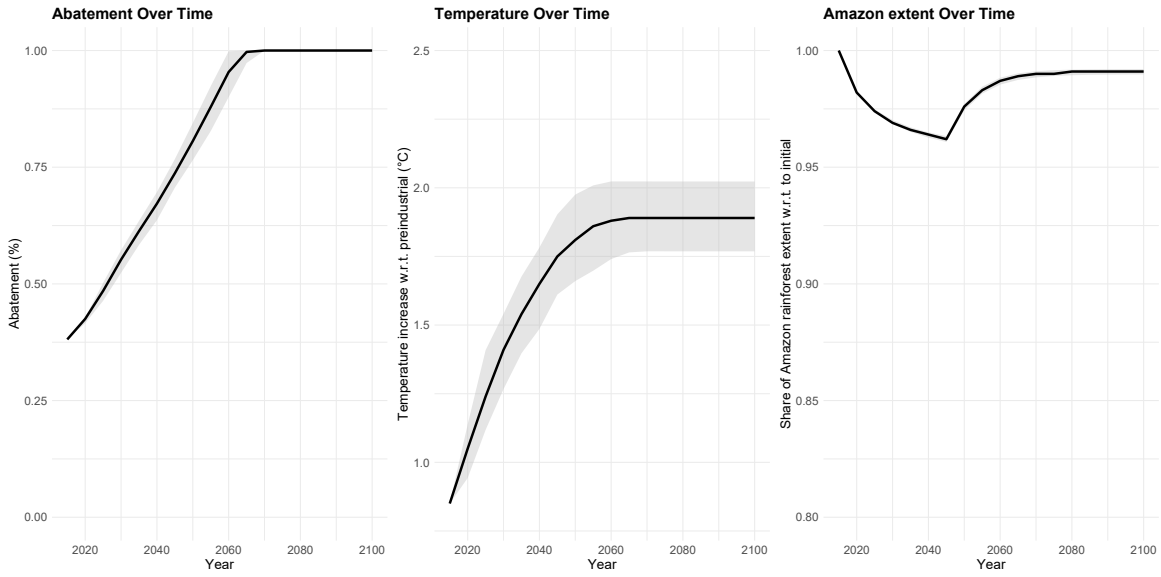

Figure 12: Stochastic optimized paths under aggregate climate risk, with endogenous amazon dynamics, with amazon idiosyncratic risk.

References

Agency, E. P. (2022). Report on the social cost of greenhouse gases: Estimates incorporating recent scientific advances. 25

Aguiar, A. P. D., I. C. G. Vieira, T. O. Assis, E. L. Dalla-Nora, P. M. Toledo, R. A. Oliveira Santos-Junior, M. Batistella, A. S. Coelho, E. K. Savaget, L. E. O. C. Aragão, et al. (2016). Land use change emission scenarios: anticipating a forest transition process in the brazilian amazon. *Global change biology 22*(5), 1821–1840. 5, 20, 37

Anderson, L. O., G. Ribeiro Neto, A. P. Cunha, M. G. Fonseca, Y. Mendes de Moura, R. Dalagnol, F. H. Wagner, and L. E. O. e. C. de Aragão (2018). Vulnerability of amazonian forests to repeated droughts. *Philosophical Transactions of the Royal Society B: Biological Sciences 373*(1760), 20170411. 2

Araujo, R., F. Costa, and M. Sant'Anna (2020). Efficient forestation in the brazilian amazon: Evidence from a dynamic model. 4, 28

Armstrong McKay, D. I., A. Staal, J. F. Abrams, R. Winkelmann, B. Sakschewski, S. Loriani, I. Fetzer, S. E. Cornell, J. Rockström, and T. M. Lenton (2022). Exceeding 1.5 c global warming could trigger multiple climate tipping points. *Science 377*(6611), eabn7950. 2, 3, 7, 14, 15, 19, 40

Baccini, A., S. Goetz, W. Walker, N. Laporte, M. Sun, D. Sulla-Menashe, J. Hackler, P. Beck, R. Dubayah, M. Friedl, et al. (2012). Estimated carbon dioxide emissions from tropical deforestation improved by carbon-density maps. *Nature climate change 2*(3), 182–185. 39

Balboni, C., A. Berman, R. Burgess, and B. A. Olken (2023). The economics of tropical deforestation. *Annual Review of Economics 15*, 723–754. 4, 7

Barnett, M., W. Brock, and L. P. Hansen (2020). Pricing uncertainty induced by climate change. *The Review of Financial Studies 33*(3), 1024–1066. 5, 7, 19

Barnett, M., W. Brock, and L. P. Hansen (2022). Climate change uncertainty spillover in the macroeconomy. *NBER Macroeconomics Annual 36*(1), 253–320. 7

Barr, J. L. and A. S. Manne (1967). Numerical experiments with a finite horizon planning model. *Indian Economic Review 2*(1), 1–31. 36

Berger, L. and V. Bosetti (2020). Are policymakers ambiguity averse? *The Economic Journal 130*(626), 331–355. 10

Berger, L., J. Emmerling, and M. Tavoni (2017). Managing catastrophic climate risks under model uncertainty aversion. *Management Science 63*(3), 749–765. 5, 7, 11, 29

Biggs, R., S. R. Carpenter, and W. A. Brock (2009). Turning back from the brink: detecting an impending regime shift in time to avert it. *Proceedings of the National academy of Sciences 106*(3), 826–831. 28

Brumm, J. and S. Scheidegger (2017). Using adaptive sparse grids to solve high-dimensional dynamic models. *Econometrica 85*(5), 1575–1612. 36

Cai, Y. (2019). Computational methods in environmental and resource economics. *Annual Review of Resource Economics 11*, 59–82. 7, 18

Cai, Y., T. M. Lenton, and T. S. Lontzek (2016). Risk of multiple interacting tipping points should encourage rapid co2 emission reduction. *Nature Climate Change 6*(5), 520–525. 8, 24

Cai, Y. and T. S. Lontzek (2019). The social cost of carbon with economic and climate risks. *Journal of Political Economy 127*(6), 2684–2734. 2, 6, 7, 8, 28

Dietz, S., C. Gollier, and L. Kessler (2018). The climate beta. *Journal of Environmental Economics and Management 87*, 258–274. 3, 6, 14

Dietz, S., J. Rising, T. Stoerk, and G. Wagner (2021). Economic impacts of tipping points in the climate system. *Proceedings of the National Academy of Sciences 118*(34). 6, 8, 9, 24

Dietz, S., F. Van Der Ploeg, A. Rezai, and F. Venmans (2021). Are economists getting climate dynamics right and does it matter? *Journal of the Association of Environmental and Resource Economists 8*(5), 895–921. 6

Dietz, S. and F. Venmans (2019). Cumulative carbon emissions and economic policy: in search of general principles. *Journal of Environmental Economics and Management 96*, 108–129. 19

Doughty, C. E., J. M. Keany, B. C. Wiebe, C. Rey-Sanchez, K. R. Carter, K. B. Middleby, A. W. Cheesman, M. L. Goulden, H. R. da Rocha, S. D. Miller, et al. (2023). Tropical forests are approaching critical temperature thresholds. *Nature*, 1–7. 16

Driscoll, J. C. and A. C. Kraay (1998). Consistent covariance matrix estimation with spatially dependent panel data. *Review of economics and statistics 80*(4), 549–560. 21, 39

Ellsberg, D. (1961). Risk, ambiguity, and the savage axioms. *The quarterly journal of economics*, 643–669. 10

Fillon, R., C. Guivarch, and N. Taconet (2023). Optimal climate policy under tipping risk and temporal risk aversion. *Journal of Environmental Economics and Management 121*, 102850. 6, 17

Flores, B. M., E. Montoya, B. Sakschewski, N. Nascimento, A. Staal, R. A. Betts, C. Levis, D. M. Lapola, A. Esquível-Muelbert, C. Jakovac, et al. (2024). Critical transitions in the amazon forest system. *Nature 626*(7999), 555–564. 5

Folini, D., F. Kübler, A. Malova, and S. Scheidegger (2024). The climate in climate economics. *Review of Economic Studies*. 2

Friedlingstein, P., M. O'sullivan, M. W. Jones, R. M. Andrew, D. C. Bakker, J. Hauck, P. Landschützer, C. Le Quéré, I. T. Luijkx, G. P. Peters, et al. (2023). Global carbon budget 2023. *Earth System Science Data 15*(12), 5301–5369. 25

Golosov, M., J. Hassler, P. Krusell, and A. Tsyvinski (2014). Optimal taxes on fossil fuel in general equilibrium. *Econometrica 82*(1), 41–88. 2, 10

Guivarch, C. and A. Pottier (2018). Climate damage on production or on growth: what impact on the social cost of carbon? *Environmental Modeling & Assessment 23*(2), 117–130. 17

Hansen, L. and T. J. Sargent (2001). Robust control and model uncertainty. *American Economic Review 91*(2), 60–66. 11

Hayashi, T. and J. Miao (2011). Intertemporal substitution and recursive smooth ambiguity preferences. *Theoretical Economics 6*(3), 423–472. 8, 11

Hong, H., N. Wang, and J. Yang (2023). Mitigating disaster risks in the age of climate change. *Econometrica 91*(5), 1763–1802. 7

Hsiao, A. (2021). Coordination and commitment in international climate action: evidence from palm oil. *Job market paper*. 4

Izhakian, Y. (2020). A theoretical foundation of ambiguity measurement. *Journal of Economic Theory 187*, 105001. 14

Ju, N. and J. Miao (2012). Ambiguity, learning, and asset returns. *Econometrica 80*(2), 559–591. 28

Keen, S., T. M. Lenton, T. J. Garrett, J. W. Rae, B. P. Hanley, and M. Grasselli (2022). Estimates of economic and environmental damages from tipping points cannot be reconciled with the scientific literature. *Proceedings of the National Academy of Sciences 119*(21), e2117308119. 7

Kent, C., R. Chadwick, and D. P. Rowell (2015). Understanding uncertainties in future projections of seasonal tropical precipitation. *Journal of Climate 28*(11), 4390–4413. 5

Klibanoff, P., M. Marinacci, and S. Mukerji (2005). A smooth model of decision making under ambiguity. *Econometrica 73*(6), 1849–1892. 8

Kriegler, E., J. W. Hall, H. Held, R. Dawson, and H. J. Schellnhuber (2009). Imprecise probability assessment of tipping points in the climate system. *Proceedings of the national Academy of Sciences 106*(13), 5041–5046. 5, 20, 22, 37, 41

Leduc, M., H. D. Matthews, and R. de Elía (2016). Regional estimates of the transient climate response to cumulative co2 emissions. *Nature Climate Change 6*(5), 474–478. 19, 21, 41

Lemoine, D. (2021). The climate risk premium: how uncertainty affects the social cost of carbon. *Journal of the Association of Environmental and Resource Economists 8*(1), 27–57. 3, 6, 13, 14, 35

Lemoine, D. and I. Rudik (2017). Managing climate change under uncertainty: Recursive integrated assessment at an inflection point. *Annual Review of Resource Economics 9*, 117–142. 13, 35

Lemoine, D. and C. Traeger (2014). Watch your step: optimal policy in a tipping climate. *American Economic Journal: Economic Policy 6*(1), 137–66. 6

Levin, S., T. Xepapadeas, A.-S. Crépin, J. Norberg, A. De Zeeuw, C. Folke, T. Hughes, K. Arrow, S. Barrett, G. Daily, et al. (2013). Social-ecological systems as complex adaptive systems: modeling and policy implications. *Environment and development economics 18*(2), 111–132. 6

Lovejoy, T. E. and C. Nobre (2019). Amazon tipping point: Last chance for action. 4

Lucas Jr, R. E. (1978). Asset prices in an exchange economy. *Econometrica: journal of the Econometric Society*, 1429–1445. 14

Malhi, Y., D. Wood, T. R. Baker, J. Wright, O. L. Phillips, T. Cochrane, P. Meir, J. Chave, S. Almeida, L. Arroyo, et al. (2006). The regional variation of aboveground live biomass in old-growth amazonian forests. *Global Change Biology 12*(7), 1107–1138. 4

Masson-Delmotte, V., P. Zhai, A. Pirani, S. L. Connors, C. Péan, S. Berger, N. Caud, Y. Chen, L. Goldfarb, M. Gomis, et al. (2021). Climate change 2021: the physical science basis. *Contribution of working group I to the sixth assessment report of the intergovernmental panel on climate change 2*. 4, 41

Matricardi, E. A. T., D. L. Skole, O. B. Costa, M. A. Pedlowski, J. H. Samek, and E. P. Miguel (2020). Long-term forest degradation surpasses deforestation in the brazilian amazon. *Science 369*(6509), 1378–1382. 5, 20

Millner, A., S. Dietz, and G. Heal (2013). Scientific ambiguity and climate policy. *Environmental and Resource Economics 55*(1), 21–46. 29

Nordhaus, W. (2018). Evolution of modeling of the economics of global warming: changes in the dice model, 1992–2017. *Climatic change 148*(4), 623–640. 18

Nordhaus, W. (2019). Economics of the disintegration of the greenland ice sheet. *Proceedings of the National Academy of Sciences 116*(25), 12261–12269. 6, 9

Papastefanou, P., C. S. Zang, Z. Angelov, A. A. de Castro, J. C. Jimenez, L. F. C. De Rezende, R. Ruscica, B. Sakschewski, A. Sörensson, K. Thonicke, et al. (2020). Quantifying the spatial extent and intensity of recent extreme drought events in the amazon rainforest and their impacts on the carbon cycle. *Biogeosciences Discussions*, 1–37. 38

Phillips, O. L., L. E. Aragão, S. L. Lewis, J. B. Fisher, J. Lloyd, G. López-González, Y. Malhi, A. Monteagudo, J. Peacock, C. A. Quesada, et al. (2009). Drought sensitivity of the amazon rainforest. *Science 323*(5919), 1344–1347. 4, 5, 21, 38, 39, 40, 42

Ritchie, P. D., J. J. Clarke, P. M. Cox, and C. Huntingford (2021). Overshooting tipping point thresholds in a changing climate. *Nature 592*(7855), 517–523. 5, 7, 9, 19, 41, 42

Rudik, I. (2020). Optimal climate policy when damages are unknown. *American Economic Journal: Economic Policy 12*(2), 340–73. 29

Sakschewski, B., W. Von Bloh, A. Boit, L. Poorter, M. Peña-Claros, J. Heinke, J. Joshi, and K. Thonicke (2016). Resilience of amazon forests emerges from plant trait diversity. *Nature climate change 6*(11), 1032–1036. 16

Scheffer, M., J. Bascompte, W. A. Brock, V. Brovkin, S. R. Carpenter, V. Dakos, H. Held, E. H. Van Nes, M. Rietkerk, and G. Sugihara (2009). Early-warning signals for critical transitions. *Nature 461*(7260), 53–59. 28

Silva-Souza, K. J. and A. F. Souza (2020). Woody plant subregions of the amazon forest. *Journal of Ecology 108*(6), 2321–2335. 21, 38, 40

Silvério, D. V., P. M. Brando, M. N. Macedo, P. S. Beck, M. Bustamante, and M. T. Coe (2015). Agricultural expansion dominates climate changes in southeastern amazonia: the overlooked non-ghg forcing. *Environmental Research Letters 10*(10), 104015. 41

Smith, C., Z. Nicholls, K. Armour, W. Collins, a. M. M. P. Forster, M. Palmer, and M. Watanabe (2021). 2021: The earth's energy budget, climate feedbacks, and climate sensitivity supplementary material. in climate change 2021: The physical science basis. *Contribution of working group I to the sixth assessment report of the intergovernmental panel on climate change 2*. 41

Souza-Rodrigues, E. (2019). Deforestation in the amazon: A unified framework for estimation and policy analysis. *The Review of Economic Studies 86*(6), 2713–2744. 4, 40

Staal, A., I. Fetzer, L. Wang-Erlandsson, J. H. Bosmans, S. C. Dekker, E. H. van Nes, J. Rockström, and O. A. Tuinenburg (2020). Hysteresis of tropical forests in the 21st century. *Nature communications 11*(1), 4978. 32

Strzalecki, T. (2013). Temporal resolution of uncertainty and recursive models of ambiguity aversion. *Econometrica 81*(3), 1039–1074. 35

Taconet, N., C. Guivarch, and A. Pottier (2021). Social cost of carbon under stochastic tipping points. *Environmental and Resource Economics 78*(4), 709–737. 17

Van den Bremer, T. S. and F. Van der Ploeg (2021). The risk-adjusted carbon price. *American Economic Review 111*(9), 2782–2810. 3, 7, 14

Yao, Y., P. Ciais, N. Viovy, E. Joetzjer, and J. Chave (2022). How drought events during the last century have impacted biomass carbon in amazonian rainforests. *Global Change Biology*. 4, 5, 21

Zemp, D., C.-F. Schleussner, H. Barbosa, and A. Rammig (2017). Deforestation effects on amazon forest resilience. *Geophysical Research Letters 44*(12), 6182–6190. 2

Zemp, D. C., C.-F. Schleussner, H. M. Barbosa, M. Hirota, V. Montade, G. Sampaio, A. Staal, L. Wang-Erlandsson, and A. Rammig (2017). Self-amplified amazon forest loss due to vegetation-atmosphere feedbacks. *Nature communications 8*(1), 1–10. 4